RENEWABLE INTEGRATION STRATEGIES FOR DATA CENTERS: OPPORTUNITIES AND CHALLENGES FOR EFFICIENCY AND SCALABILITY

Lappeenranta–Lahti University of Technology LUT

Master's thesis

Master's programme in Electrical Engineering

2026

Ummay Afrina Jahan Sutapa

Examiner(s): Professor, Behnam Mohammadi-Ivatloo

Junior Researcher, Mohammad Seyfi

ABSTRACT

Lappeenranta–Lahti University of Technology LUT

LUT School of Energy Systems

Electrical Engineering

Ummay Afrina Jahan Sutapa

Renewable Integration Strategies for Data Centers: Opportunities and Challenges for Efficiency and Scalability

Master's thesis

2026

75 pages, 10 figures and 9 tables

Examiner(s): Professor, Behnam Mohammadi-Ivatloo, Junior Researcher, Mohammad Seyfi

Keywords: Data center, renewable energy integration, battery energy storage, workload flexibility, energy optimization, scalability.

The thesis investigates the way in which renewable energy, battery storage, UPS operation, and flexible IT workloads can be combined in a grid-connected data center to reduce the grid electricity consumption and to use renewable energy efficiently. An hourly operational optimization model was developed using Python and Pyomo and then simulated for the whole year of 2025 based on weather data which was obtained from the Finnish Meteorological Institute. The model considers photovoltaic and wind power generation, battery storage, UPS operation, both flexible and non-flexible IT workloads, cooling demand, and grid electricity. Six operating scenarios were analyzed by varying renewable-generation capacity, battery capacity and the permitted level of workload flexibility. Their effects on grid electricity consumption, renewable-energy utilization, storage operation and workload scheduling were then evaluated.

The results show that the largest reduction in grid electricity imports occurs when renewable-generation capacity is increased. A larger battery is most useful when sufficient surplus renewable electricity is available for charging. In high-renewable scenarios, shifting flexible workloads reduces grid electricity use and enables more of the available renewable energy to be utilized. The study finds that for renewables to be effectively and massively used in the data centers, they need to be balanced with flexible demand, renewable generation and storage capacity. Instead of increasing each of these elements independently, they must all be raised simultaneously.

ACKNOWLEDGEMENTS

I would like to express my sincere gratitude to Professor Behnam Mohammadi-Ivatloo for his valuable guidance, expertise and support throughout this thesis. I am also deeply grateful to my supervisor, Mohammad Seyfi, for his continuous guidance, constructive feedback, patience and encouragement during the development of this work. Their support played an important role in completing this thesis.

I owe heartfelt thanks to my parents and my elder brother, whose countless sacrifices and unconditional support in me have brought me to where I am today. This journey was possible only because of their relentless dedication. Everyone in my family deserves endless appreciation for always offering me warmth and encouragement whenever I struggle through the difficulties of this degree.

My special thanks go to my friend Nafisa, who stuck with me through every high and low of being a master's student. I would also like to express my endless gratitude to my friends Irin and Ashik, who showed up for me from the very first day, without ever needing to be asked.

This thesis is dedicated to my parents, who have been my constant source of strength and inspiration. Their belief in me has never faltered and has allowed me to reach this far. This achievement belongs to them as much as it does to me.

SYMBOLS AND ABBREVIATIONS

Roman characters

AT	Ambient temperature	°C
Cap	Energy-storage capacity	kWh
D	Maximum allowable workload delay	h
E	Stored energy in storage units	kWh
I	Electric current	A
J	Total grid electricity imported	kWh
K_i	Temperature coefficient of PV current	A/°C
K_v	Temperature coefficient of PV voltage	V/°C
NOT	Nominal operating temperature	°C
P	Electrical power	kW
p	Power in the battery formulation	kW
s	Flexible-workload arrival-time index	
sor	Solar irradiance	kW/m²
T	Total number of simulation time steps	
TC	PV cell temperature	°C
t	Time index	
V	Voltage	V
V^W	Wind speed	m/s
x	Scheduled flexible-workload energy	kWh

Greek characters

Δt	Simulation time step	h
η^{ESS}	Battery storage system efficiency	
$\eta_{ch}{}^{UPS}$	UPS charging efficiency	
$\eta_{disch}{}^{UPS}$	UPS discharging efficiency	
$\eta_{B,ch}$	Charging efficiency of the battery	
$\eta_{B,dis}$	Discharging efficiency of the battery	
$\eta_{UPS,ch}$	UPS charging efficiency in the operational model	

$\eta_{\mathrm{UPS,dis}}$	UPS discharging efficiency in the operational model
θ	Scenario index

Dimensionless quantities

FF	PV module fill factor
k_{cool}	Cooling-to-IT power coefficient
$Loss^{\mathrm{ESS}}$	Battery cycling-loss coefficient in the literature-based formulation
$Loss_{\mathrm{B}}$	Battery cycling-loss coefficient in the operational formulation
N^{PV}	Number of PV modules
PUE	Power usage effectiveness
$\mathrm{SoC}_{\mathrm{min}}$	Minimum allowable UPS state of charge
$\mathrm{SoC}_{\mathrm{max}}$	Maximum allowable UPS state of charge
u_t	CPU utilization fraction at time t
$u_{B,t}$	Binary battery operating-mode variable
$u_{UPS,t}$	Binary UPS operating-mode variable
$z_{ch,t}^{UPS}$	Binary UPS charging-status variable
$z_{disch,t}^{UPS}$	Binary UPS discharging-status variable

Subscripts

arrival	Workload arrival
B	Battery
base	Rated or base value
BCW	Building chilled-water system
ch	Charging
chiller	Chiller
ci	Cut-in wind speed
co	Cut-out wind speed
cool	Cooling demand
cooling	Total cooling power
CRAH	Computer room air-handling unit
CT	Cooling tower

curt	Renewable curtailment
dch	Battery discharging in the literature-based formulation
dis	Discharging in the operational formulation
disch	UPS discharging in the literature-based formulation
end	End of the optimization period
flex	Flexible workload
grid	Grid electricity or grid-power flow
idle	Idle operating condition
IT	Information-technology load or equipment
load	Data-center electrical load
max	Maximum value
min	Minimum value
MPP	Maximum power point
net	Net power exchange
nonflex	Non-flexible workload
OC	Open circuit
other	Other facility components
PV	Photovoltaic source
r	Rated wind value
rack	Rack or server fans
ren	Renewable power
reserve	Minimum UPS stored-energy reserve
sch	Scheduled workload
SC	Short circuit
start	Beginning of the optimization period
tot	Total
UPS	Uninterruptible power supply
WT	Wind-turbine generation
→	Direction of power flow from the source on the left to the destination on the right

Superscripts

cooling	Cooling-power term
ESS	Energy storage system
ext	Extended time horizon

grid	Grid-import power
initial	Initial stored-energy value
IT	Information-technology workload
max	Maximum value
PV	Photovoltaic-generation quantity
UPS	Uninterruptible power supply
W	Wind-speed variable
wind	Wind-turbine power generation

Abbreviations

AI	Artificial intelligence
BCW	Building chilled water
CBC	COIN-OR Branch and Cut
CPU	Central processing unit
CRAH	Computer room air handling unit
CT	Cooling tower
EMS	Energy management system
ESS	Energy storage system
FMI	Finnish Meteorological Institute
HRES	Hybrid renewable energy systems
IT	Information technology
MILP	Mixed-integer linear programming
PDU	Power distribution unit
PUE	Power usage effectiveness
PV	Photovoltaic
RES	Renewable energy sources
STC	Standard Test Conditions
UPS	Uninterruptible power supply

Table of contents

Abstract

(Acknowledgements)

(Symbols and abbreviations)

Declarations

1 Introduction 13
1.1 Background and motivation 13
1.2 Research problem and objectives 14
1.3 Scope and limitations 15
1.4 Structure of the thesis 16
2 Literature review 17
2.1 Data center energy use and sustainability trends 17
2.2 Overview of renewable integration strategies 18
2.2.1 Hybrid renewable energy systems (HRES) 18
2.2.2 Advanced energy-management systems 19
2.2.3 Energy management, optimization, and scheduling for data center flexibility 19
2.2.4 Multi-energy integration 20
2.2.5 Grid-interactive data center flexibility 20
2.3 Challenges and gaps in current approaches 21
2.3.1 Intermittency and reliability constraints 21
2.3.2 Limitations in optimization under uncertainty 21
2.3.3 Scalability and EMS complexity 22
2.3.4 Underutilization of flexibility resources 22
3 Methodology 23
3.1 Methodological framework 23
3.2 Data sources and modeling assumptions 23
3.2.1 Workload flexibility 24
3.2.2 UPS and battery-based flexibility 24

3.2.3 Scope of assumptions....25
3.3 System description....26
3.4 Mathematical formulation....29
3.4.1 Photovoltaic power generation model....29
3.4.2 Wind turbine power generation model....31
3.4.3 IT workload flexibility equation....32
3.4.4 IT workload scheduling and demand preservation....33
3.4.5 Battery storage system....34
3.4.6 UPS energy and net power formulation....35
3.4.7 Total cooling power and power-balance formulation....39
3.5 Operational objective function....41
3.6 Operational constraints....42
3.6.1 Renewable generation and power balance....43
3.6.2 Battery constraints....44
3.6.3 UPS constraints....44
3.6.4 IT workload shifting constraints....45
3.6.5 Cooling demand constraints....46
4 Simulation setup and scenario design....47
4.1 Simulation environment and time horizon....47
4.2 Simulation scenario design....48
4.3 Renewable energy resource data....49
4.4 Base-case system capacity and component assumptions....51
4.5 IT workload flexibility and computational demand preservation....53
4.6 Battery storage system specifications....53
4.7 UPS characteristics....54
4.8 Cooling system specifications....55
4.9 Model evaluation criteria....56
5 Results and discussion....57
5.1 Overall scenario performance....57
5.2 Renewable utilization and curtailment....59
5.3 Battery capacity and scalability....60
5.4 Effect of workload flexibility....62
5.5 Representative data-center operation....64

5.6 Model validation 65
6 Opportunities and challenges 67
6.1 Opportunities for efficient data center operation 67
6.2 Opportunities and challenges for system scalability 68
6.3 Challenges of renewable-integrated data center operation 68
6.4 Implications for efficient and scalable data center operation 69
7 Conclusions 70
7.1 Summary of findings 70
7.2 Study limitations 71
7.3 Future research directions 71
References 73

Figures

Figure 3.1. Schematic representation of power flows within the renewable-integrated data center system. 28
Figure 4.1. Annual photovoltaic generation profile used in the base simulation. 50
Figure 4.2. Daily mean and maximum wind generation used in the base simulation. 51
Figure 5.1. Annual grid electricity imports across the six simulation scenarios. 58
Figure 5.2. Renewable energy utilization and curtailment across the six simulation scenarios. 59
Figure 5.3. Effect of battery capacity on grid electricity import and renewable energy utilization. 61
Figure 5.4. Daily mean battery state-of-charge profiles for 1200 kWh and 3600 kWh storage capacities under the triple-renewable scenario. 62
Figure 5.5. Effect of workload shifting on monthly grid electricity import and renewable curtailment. 63
Figure 5.6. Optimized data-center electrical demand during a representative week in the base scenario. 64
Figure 5.7. Representative 24-hour optimized electrical power balance for the triple-renewable and triple-battery scenario. 65

Tables

Table 3.1. Data center flexibility characteristics reported in the literature. 25
Table 4.1. Scenario settings used for integrated optimization analysis. 48
Table 4.2. Base-case system and simulation parameters. 52
Table 4.3. IT workload profiles and flexibility settings. 53
Table 4.4. Battery storage energy, power, and efficiency parameters. 54
Table 4.5. UPS energy, power, efficiency, and operating limits. 54
Table 4.6. Parameters of the IT-load-dependent cooling model. 56
Table 5.1. Main annual results of the six simulation scenarios. 57
Table 5.2. Maximum numerical validation errors across the six simulation scenarios. 66

DECLARATIONS

Turnitin

The originality of this thesis has been reviewed with the Turnitin similarity checking service.

AI usage

The author of the thesis, Ummay Afrina Jahan Sutapa, used the following AI-tools during the preparation of the thesis:

1. ChatGPT
    a. Purpose of use: Language refinement and proofreading assistance for academic writing style.
    b. Explanation of the use of the tool: The AI tool was used to review and improve the language quality of selected sections. All technical content, calculations, modeling, analysis, and conclusions are the original work of the author.

Responsibility

The author, Ummay Afrina Jahan Sutapa, takes full responsibility for the content, calculations, results, interpretations and final discussions of this thesis. The AI tool was not used to generate research results and analysis or to replace the author's own writing. The author has reviewed the content generated by the possible use of AI tool.

1 Introduction

1.1 Background and motivation

Nowadays, the expansion of digitalization, cloud computing and data-driven services has substantially increased both the number and scale of data centers (He *et al.*, 2024; Takcı *et al.*, 2025a). Data centers require a continuous and reliable electricity supply because they operate 24 hours a day and must maintain strict power-quality and service-availability standards (Bhardwaj *et al.,* 2024). As the data centers need high power to run continuously, and their electricity usage has been gradually rising in the past few years, data centers are among the most energy-intensive forms of infrastructure (He *et al.*, 2024). The increasing rise in high energy consumption has escalated the concern about growing operating costs, a greater grid electricity reliance, and particularly carbon emissions (He *et al.*, 2024).

As a result, to reach the climate goals and to lessen the dependence on the fossil fuels, electricity distribution systems are being transitioned to low-carbon energy sources (He *et al.*, 2024; Takcı *et al.*, 2025a). For this cause, photovoltaic panels and wind turbines, which are the renewable energy technologies, are being integrated at an accelerating pace (He *et al.*, 2024). The main issue with these renewable sources is their nature of inconsistent and intermittent reliability, balancing, and the stability of the system, even though these technologies are clearly beneficial for the environment (He *et al.*, 2024). As data centers are broad and inflexible loads that need reliable and continuous power, these inconsistent renewable characteristics are acute for them, even brief power outages can have serious operational and economic effects (He *et al.*, 2024; Takcı *et al.*, 2025a).

While renewable energy integration into the power supply systems in data centers is an opportunity to maintain sustainability, it is also a challenge due to the difficult nature of their energy generation (He *et al.*, 2024). Increasing the share of renewable electricity in data-center operations can help lower carbon emissions and reduce their environmental impact. But it is difficult to achieve high renewable penetration levels while maintaining reliability which requires well-planned energy supply systems, energy storage solutions and control strategies based on the optimization (He *et al.,* 2024; Bhardwaj *et al.,* 2024). To keep their servers running, researchers and businesses are increasingly interested in renewable-

powered and grid-interactive data center energy systems (He *et al.,* 2024; Takcı *et al.,* 2025a).

1.2 Research problem and objectives

Researchers explored various methods that renewable resources could be used in data centers. One of the popular configurations involves hybrid renewable energy systems combining photovoltaic (PV) and wind power with the conventional secondary energy storage systems to increase the proportion of data center electricity demand supplied by renewable sources without compromising supply reliability (He *et al.*, 2024). Most research analyses indicate that PV-based configurations often offer fair trade-offs between renewable penetration and lower cost of electricity, whereas wind power generation alone typically provides limited benefits unless deployed in combination with solar generation (He *et al.*, 2024). Yet battery storage systems are more expensive, but they are better at renewable energy because they can adjust to short-term modifications (He *et al.*, 2024).

The main factors for integrating renewable energy are energy management systems (EMS) along with the energy supply planning into data centers. The advanced EMS optimizes and adapts to different situations (Bhardwaj *et al.,* 2024). It consumes less electricity on the grid and improves operational performance by controlling traditional power sources, battery storage and renewable generation. Besides, optimization and scheduling techniques assist data centers in altering their energy consumption trends and in making sure that computer workloads are synchronized with the times when green energy is available for free. This is suitable for demand response and makes the power system more flexible (Takcı *et al.*, 2025b).

The literature review of this thesis still identifies some of the unresolved challenges even though there are changes. One of the fundamental limitations is that renewable energy intermittency, particularly in systems which do not have optimally sized energy storage solutions (He *et al.,* 2024). The uncertainty in renewable generation, electricity prices, and data center load profiles are not taken into consideration in various optimization methods, which can reduce their robustness under real operating conditions (Fan *et al.,* 2022). The concerns about the scalability, operational reliability, and cybersecurity of the system raises because of the growing complexity of the system which integrate multi-energy sources and

advanced control strategies (Bhardwaj *et al.,* 2024). Grid-connected data centers have considerable technical potential to provide flexibility; however, flexibility services based on uninterruptible power supply (UPS) systems are not yet widely adopted because of regulatory barriers and insufficient financial incentives (Takcı *et al.,* 2025a).

This thesis addresses the research problem of how the integration of the renewable energy strategies can be implemented in data centers in a manner that improves the data center's efficiency while maintaining reliability and scalability. This thesis aims to develop and assess a simplified simulation framework for a renewable-integrated data center. The thesis examines the effects of photovoltaic and wind generation, battery capacity, UPS operation, and flexible workload scheduling on grid electricity consumption, renewable-energy utilization, renewable curtailment, storage operation, and overall system performance. The optimization model minimizes total grid electricity import while satisfying the system's technical operating constraints. The simulation outcomes are then used to identify the main opportunities and challenges associated with improving the efficiency and scalability of renewable-integrated data centers.

1.3 Scope and limitations

The scope of this study is a simulation-based evaluation of renewable-energy integration strategies for data centers. The study considers a grid-connected data center energy system supplied by solar PV, wind power, battery storage, UPS support, and electricity imported from the grid. Workload flexibility is included as a demand-side strategy to examine whether shifting part of the information technology (IT) workload can improve the use of available renewable energy.

The simulation uses hourly renewable resource data together with literature-based assumptions for data center operation, battery storage, workload flexibility, UPS characteristics, and cooling demand. The main objective is to evaluate how renewable generation, battery storage capacity, UPS operation, and workload flexibility affect annual grid electricity consumption, renewable energy utilization, renewable curtailment, storage operation, and power-balance consistency.

The study is limited to a simplified representation of a data center energy system and does not represent a measured industrial facility or a fully site-specific design. The IT load is represented using time-varying flexible and non-flexible workload profiles, while cooling demand is represented as a simplified IT-load-dependent demand with a minimum cooling requirement. The UPS is modeled as an additional controllable storage resource that must maintain a minimum energy reserve. Its operation is determined by the optimizer.

This thesis does not include detailed techno-economic optimization, battery degradation modeling, real-time control analysis, detailed cooling-system dynamics, or detailed regional regulatory assessment. Backup diesel generators are also excluded, as the focus is on renewable integration using PV, wind, battery storage, UPS operation, grid supply, and workload flexibility. These choices keep the model focused on the main research objective: evaluating how renewable generation, battery storage, workload flexibility, and limited UPS support can support data center energy operation.

1.4 Structure of the thesis

This thesis is organized into seven chapters. Chapter 1 establishes the study background, defines the research problem and objectives, and specifies the scope and limitations. Chapter 2 examines previous studies on data center electricity use, renewable integration, hybrid energy systems, energy management, workload flexibility, and grid-interactive data center operation. It also outlines the major problems and knowledge gaps related to the renewable energy integrated operation of a data center. Chapter 3 presents the research methodology that includes assumptions, system configuration, mathematical formulation, objective functions and operational constraints.

Chapter 4 discusses the simulation environment, input data, parameters of components, and scenario design. Chapter 5 shows the results from simulations that include imports from the grid, renewable energy usage, curtailment, battery scalability, workload flexibility, system operation, and model validation. Chapter 6 discusses the potential of opportunities and challenges in relation to effective and scalable renewable integrated data center operations. Finally, Chapter 7 presents the principal conclusions, discusses the study limitations, and identifies directions for further research.

2 Literature review

The worldwide expansion of digitalization and cloud computing has made data centers a major and continuously growing source of electricity demand (He *et al.,* 2024; Bhardwaj *et al.,* 2024). Their continuous operation, strict reliability requirements, and expanding computational demands have increased the interest in carbon-efficient and renewable-powered energy supply systems (Bhardwaj *et al.,* 2024; Takcı *et al.,* 2025a), especially from artificial intelligence (AI) and machine-learning applications. The decarbonization goals, related to energy security concerns, grid integration issues, and the need for operational resilience, have contributed to the academic and industrial research on hybrid renewable systems, data center adaptability, advanced EMS, and multi-energy integration (He et al., 2024; Takcı et al., 2025a).

As computational workloads and cloud-based services continue to expand, efficient energy use and optimized operation have become increasingly important for the sustainability and adaptability of data centers (Bhardwaj *et al.,* 2024). Combining renewable energy sources with intelligent scheduling and real-time load management can reduce dependence on grid electricity while enabling data centers to support power-system flexibility (He *et al.,* 2024; Takcı *et al.,* 2025a). Through optimization algorithms, EMS can forecast renewable generation, adjust electricity-consumption patterns, support participation in demand-response, enhance grid stability and reduce operating costs (Bhardwaj *et al.,* 2024).

This literature review covers data center energy use, renewable energy integration, energy storage, energy management, workload flexibility, grid-interactive operation, and the main challenges identified in earlier studies.

2.1 Data center energy use and sustainability trends

Globally, electricity consumption by data centers continues to increase, driven mainly by the expansion of cloud services, high-performance computing, and connected devices (Bhardwaj *et al.,* 2024; Takcı *et al.,* 2025a). In many small- and medium-sized facilities, power usage effectiveness (PUE) remains above optimal efficiency levels (Bhardwaj *et al.,*

2024). Bhardwaj *et al.* (2024) reports that higher demand increases dependence on grid electricity, which enhances both the operational cost and the carbon emissions.

The necessity for sustainability also creates new challenges within the power systems. (He *et al.,* 2024) the increasing share of renewable generation in national electricity systems introduces additional intermittency and balancing challenges, thereby increasing the importance of flexible loads. Takcı *et al.* (2025a) also indicate that the data centers can be used as adaptive resources to support low-carbon grids instead of being just energy consumers owing to their high load levels and available backup resources.

EMS systems in data centers can help balance power demand, renewable energy generation and storage. Bhardwaj *et al.* (2024) propose that closer coordination among these components can reduce data centers' dependence on grid electricity and improve overall energy performance. It is also becoming more relevant in the real world. Large electrical loads, including data centers, are growing rapidly and creating increasing uncertainty for power-system planning. Rickerson (2025) reports that large loads may connect within approximately 6–18 months, whereas the transmission infrastructure required to support them may take 3–6 years to develop. This difference creates significant forecasting, interconnection and transmission-planning challenges. These challenges further emphasize the importance of flexible data-center operation in supporting the transition towards low-carbon power systems (Takcı *et al.,* 2025a).

2.2 Overview of renewable integration strategies

2.2.1 Hybrid renewable energy systems (HRES)

Renewable energy sources (RES), including solar PV, wind power and hydrogen technologies, combined with battery energy storage systems, are among the most widely studied approaches for supplying data centers sustainably (He *et al.,* 2024). He *et al.* (2024) applied multi-objective optimization to a hybrid energy system for a data center and found that solar-based configurations offered the most favorable balance between cost and renewable-energy integration. Wind energy boosts efficiency when employed alongside PV, even though it has a minor independent contribution (He *et al.,* 2024).

Battery energy storage systems are a key aspect of boosting the usage of clean electricity. According to the simulation results reported by He *et al.* (2024), however, batteries drastically raise the capital expenditure; they allowed renewable incorporation up to 40-45% while retaining stability. Their outcomes underscore that in renewable-powered data centers to optimize expense, reliability, and emission reduction achievements, they strongly depend on the significance of meticulous component placement and sizing (He *et al.,* 2024).

2.2.2 Advanced energy-management systems

EMS solutions are needed in data centers to enable real-time coordination of grid imports, storage and renewable energy supply (Bhardwaj *et al.,* 2024). They have fortified the EMS framework with PV, wind generation, batteries and hydrogen storage using AI enabled predictions for load and renewable energy (Bhardwaj *et al.,* 2024). Their simulation results show that the EMS reduces grid electricity consumption by charging the batteries during periods of high solar generation and discharging them during peak-demand hours.

As an alternative prolonged option, hydrogen storage increases robustness of the system beyond conventional batteries. Bhardwaj *et al.* (2024) suggest that fuel cell batteries can help stabilize supply when the renewable generation is less, while hydrogen electrolysis systems can convert additional renewable energy into storable power, enabling an attractive alternative for vital facilities.

2.2.3 Energy management, optimization, and scheduling for data center flexibility

EMS systems coordinate demand, renewable generation, energy storage and grid electricity in data centers. Optimization can determine when to store energy, when to use it and when to get it from the grid. It can also facilitate demand response by shifting the time of suitable computer-related tasks (Takcı *et al.,* 2025a; Bhardwaj *et al.,* 2024).

Data-center workloads can generally be divided into delay-sensitive and delay-tolerant tasks. Delay-sensitive tasks must be processed immediately, whereas delay-tolerant tasks may be shifted within a limited period without affecting service requirements (Zhao and Wang, 2021). This allows to shift some of the power needs to times when there is more renewable energy or less demand on the grid (Takcı *et al.,* 2025b). If more renewable generation is

available, it can be stored and used later when there is less renewable energy available (Takcı *et al.,* 2025a; Bhardwaj *et al.,* 2024). To cope with such fluctuations of supply and demand, some EMS systems use a combination of load estimation, renewable-generation forecasting and efficient optimization (Bhardwaj *et al.,* 2024).

Nonetheless, in many studies, workload flexibility and renewable energy are still being studied independently. Bhardwaj *et al.* (2024) consider renewable generation, storage and grid interaction in their study but do not include flexible IT workloads. Takcı *et al.* (2025b), however, consider workload flexibility and demand response, but do not directly combine them with on-site renewable generation. This shows that the full potential of the joint use of renewable generation, storage, UPS systems, and flexible workloads is not yet explored. Electricity pricing, peak-demand management, and advanced forecasting are not considered in this study. Instead, the final model coordinates renewable generation, battery storage, UPS operation, and flexible IT workloads while minimizing total grid electricity import.

2.2.4 Multi-energy integration

Multi-energy integration combines different energy carriers, renewable generation, energy-conversion technologies and storage within a coordinated system (Aljabery *et al.,* 2021). Energy hubs enhance operational flexibility, supply reliability and overall efficiency by coordinating electricity, heating, cooling, gas and other energy flows (Aljabery *et al.,* 2021). Their operation, however, is influenced by variations in renewable generation, energy prices and demand, which can be addressed using suitable uncertainty-modeling and optimization methods (Fan *et al.,* 2022).

2.2.5 Grid-interactive data center flexibility

Modern data centers can help the power grid by using UPS systems, demand response and workload shifting. Takcı *et al.* (2025a) point out that these resources can convert data centers into virtual energy storage and offer services such as frequency response. Mitra (2025) explains that double-conversion UPS systems are generally independent of input-voltage and frequency changes and that control of their converter and battery systems can significantly influence grid behavior. The front-end control of the UPS is therefore particularly important

when modeling data center loads for grid stability studies. However, gaps in interconnection requirements, coordination practices, ride-through requirements, load modeling and reliability standards remain important implementation challenges (Springer *et al.,* 2025).

However, most studies focus on grid services and often study workload flexibility, UPS operation, and on-site renewable generation separately (Takcı *et al.,* 2025a). Therefore, their joint operation has not been studied extensively yet. For the purpose of this thesis the UPS is not used for frequency response or other grid services. It is modeled as a controllable storage resource with a minimum energy reserve to be maintained.

2.3 Challenges and gaps in current approaches

Encouraging growth is still being hindered by several key challenges for the widespread adoption of renewable-energy-powered data centers (He *et al.,* 2024; Bhardwaj *et al.,* 2024).

2.3.1 Intermittency and reliability constraints

The variable output of solar and wind generation remains a major obstacle to large-scale renewable-energy deployment (He *et al.,* 2024). Batteries and hydrogen storage alleviate this problem, but He *et al.* (2024) point out that the storage capacity needs to be optimized accurately to ensure both high reliability and renewable turnover, which may be prohibitively expensive.

2.3.2 Limitations in optimization under uncertainty

The uncertainties of renewable generation, the load forecast, the operation of the equipment and the energy prices and market conditions have an influence on integrated energy systems (Fan *et al.,* 2022). These uncertainties can be modeled with stochastic and robust optimization methods, but each method has different requirements and limitations (Fan *et al.,* 2022). This thesis does not explicitly model the uncertainty, but renewable generation is evaluated based on one year of weather data and pre-defined workload profiles.

2.3.3 Scalability and EMS complexity

Multi-energy structures are getting more complex to be managed for EMS frameworks (Bhardwaj *et al.,* 2024). The use of AI-based estimation, hydrogen storage and multi-vector dispatch raise the operational and cybersecurity threats' complexity as noted by Bhardwaj *et al.* (2024). However, scaling such systems to large multi-site data center networks (Bhardwaj *et al.,* 2024) is still a challenge.

To study scalability, in this thesis, the renewable-generation and battery-storage capacities are varied in a representative data center. The study does not consider multi-site data center expansion and geographical workload migration.

2.3.4 Underutilization of flexibility resources

Even though data center adaptability is well-defined, there is yet insufficient practical use for it (Takcı *et al.,* 2025a). Takcı *et al.* (2025a) identify that regulatory obstacles and the shortage of financial incentives are the main causes of the lack of widespread acceptance of UPS-based services and workload shifting.

The literature also reveals a lack of simple, integrated modeling approaches for considering on-site renewable generation, energy storage, UPS operation, and workload flexibility in data center energy management. A large number of works dedicated to renewables assume inflexible data center loads (He *et al.,* 2024), while flexibility-oriented works tend to ignore explicit modeling of on-site renewable generation (Takcı *et al.,* 2025b). This separation limits the ability to assess the degree of operational flexibility in aligning flexible workloads to variable renewable energy availability.

These gaps motivate the need for a simplified and scalable data center energy management framework that jointly considers renewable energy availability, storage operation, UPS reserve requirements, and flexible workload scheduling.

3 Methodology

This chapter presents the methodological approach adopted to evaluate renewable energy integration in a grid-connected data center. We use literature-based data center models and parameters, hourly meteorological data and mathematical optimization to evaluate the interaction of renewable generation, energy storage, IT workload flexibility, cooling demand and grid electricity.

This chapter describes the methodological framework, modeling assumptions, system configuration, mathematical formulation, operational objective and constraints. Chapter 4 presents the detailed simulation setup and scenario design.

3.1 Methodological framework

This thesis follows a model-based analytical approach supported by mathematical optimization. A representative data center model is developed using parameters and component models from published literature together with hourly meteorological observations for renewable generation.

The model integrates photovoltaic and wind generation, battery storage, UPS operation, flexible and non-flexible IT workloads, cooling demand, and grid electricity. Flexible workloads may be shifted within an allowable delay period, while non-flexible workloads are processed immediately.

The optimization coordinates these components over hourly time steps while satisfying the operational constraints of the system. The same modeling framework is applied to different scenarios to evaluate grid electricity dependence, renewable energy utilization, curtailment, storage operation, workload flexibility, and system scalability.

3.2 Data sources and modeling assumptions

The modeling assumptions in this thesis are mainly based on published academic studies and the renewable resource inputs are based on hourly meteorological data from the Finnish

Meteorological Institute (FMI). This allows for the integration of literature-based data center parameters with time-varying solar radiation, temperature and wind-speed data. The assumptions about data center flexibility are mostly based on Takcı *et al.* (2025a) and Takcı *et al.* (2025b) that offer a foundation for modeling the workload flexibility, UPS operation, and other operational characteristics without requiring proprietary data.

3.2.1 Workload flexibility

Workload flexibility is defined as the ability to shift a portion of data center computing tasks in time without violating their processing requirements. Data center workloads can contain both delay-sensitive tasks that require immediate processing and flexible tasks that can be shifted within a limited time window (Takcı *et al.,* 2025a; Takcı *et al.,* 2025b).

In this thesis, the IT workload is therefore divided into flexible and non-flexible components using time-varying hourly workload profiles. Non-flexible workload is processed in the hour in which it arrives, whereas flexible workload may be rescheduled within the allowed delay window. The base simulation allows a maximum delay of 3 hours, while all computational workload must still be completed. The installed IT processing capacity is limited by a maximum capacity parameter. The detailed workload profiles and numerical simulation parameters are presented in Chapter 4.

3.2.2 UPS and battery-based flexibility

Besides workload flexibility, this thesis presents battery storage as a short-term energy management component. The battery may be charged from available renewable generation or grid electricity, while its charging and discharging operation is determined by the optimization model subject to its energy, power, efficiency, and operating constraints. Battery discharge can reduce grid electricity imports when stored energy is available. This enables an assessment of whether battery storage can enhance renewable energy utilization, decrease curtailment, and reduce grid electricity imports.

The UPS is not part of battery storage. In actual data centers, UPS systems are mainly used for protecting critical loads during power disturbances and providing short-term backup power before other backup systems are online. Previous studies show that UPS systems can

be used for flexibility applications; however, their implementation is limited by reliability requirements and operational constraints (Takcı *et al.,* 2025a; Takcı *et al.,* 2025b).

In this thesis, the UPS is included as an additional controllable storage resource while retaining a minimum energy reserve. Its charging and discharging decisions are determined by the optimization model subject to its energy capacity, reserve level, charging and discharging power limits, and efficiency constraints. The UPS is not restricted to predefined renewable-deficit hours, and no additional penalty is applied to UPS discharge in the final operational optimization. This allows the model to evaluate the interaction between renewable generation, battery storage, UPS operation, grid supply, and workload flexibility without predetermining the storage dispatch decisions.

3.2.3 Scope of assumptions

To keep the model clear and focused, only the main flexibility options discussed in the selected literature are considered in this thesis. These include IT workload shifting, battery storage, and UPS operation, based mainly on Takcı *et al.* (2025a) and Takcı *et al.* (2025b). Other flexibility options, such as dynamic cooling control or geographical workload shifting, are not included in the model.

The principal flexibility characteristics identified in previous studies are presented in Table 3.1, whereas the numerical parameters adopted for the simulation are provided in Chapter 4.

Table 3.1. Data center flexibility characteristics reported in the literature.

Flexibility source	Description	Evidence from literature	Reference
Workload flexibility	Data center workloads include time-critical tasks and tasks that can tolerate postponement. Tasks in the latter category may be rescheduled without breaching service requirements.	Workload scheduling and load shifting are important flexibility options in data centers.	(Takcı *et al.,* 2025a)
Load shifting capability	Data centers can change the timing of electricity use by shifting flexible computing tasks.	Load shifting is one of the main flexibility mechanisms available in data centers.	(Takcı *et al.,* 2025b)
Flexibility characteristics	Data center flexibility can be described using factors such as magnitude, activation time, duration, and recovery time.	These characteristics are used to describe the flexibility potential of different data center resources.	(Takcı *et al.,* 2025b)

UPS-based flexibility	UPS systems are mainly used for reliability, but they can also provide short-term flexibility when operated within their technical limits. The UPS is included in the operational model used in this thesis.	UPS systems can provide short-duration flexibility services to the power system.	(Takcı *et al.,* 2025a; Takcı *et al.,* 2025b)

Table 3.1 summarizes the principal flexibility options identified in previous studies. Takcı *et al.* (2025a) and Takcı *et al.* (2025b) show that workload shifting and UPS systems can provide significant operational flexibility in data centers. In this thesis, the workload flexibility is modeled by delaying delay-tolerant tasks within a given time window. Energy-storage resources include battery storage and the UPS, subject to their operating limits. Other flexibility options, in particular dynamic cooling control, are not included in this study.

3.3 System description

The system examined in this thesis is a grid-connected data center that includes on-site photovoltaic and wind generation, battery energy storage, and UPS support. IT workloads and cooling requirements are the main drivers of the data center's electricity demand. The model examines the interactions among variable renewable generation, battery and UPS operation, and flexible data-center demand, consistent with the research gap identified in Chapter 2.

The data center is not modeled as one inflexible load according to the component-based flexibility framework proposed by Takcı *et al.* (2025a). Instead, its electricity demand is divided into components with different flexibility characteristics. In this study, flexibility is mainly provided through IT workload scheduling. The battery is used as the main storage component, while the UPS is modeled separately and must remain within its energy and minimum reserve limits. Both storage systems are operated by the optimization model subject to their technical constraints. Cooling power consumption is included as part of the data center demand, while detailed cooling flexibility, such as thermal inertia or dynamic cooling control, is not considered.

The hourly IT workload arrivals are treated as input data based on predefined flexible and non-flexible workload profiles. The resulting IT power demand depends on the immediate

processing of non-flexible workload and the scheduling of flexible workload, while the total IT power is limited by the installed IT-capacity constraint. The workload is divided into:

- Non-flexible (delay-sensitive) workload, which must be processed immediately, and
- Flexible (delay-tolerant) workload, which can be deferred and rescheduled within a bounded time window.

This classification is according to the workload flexibility as mentioned by Takcı *et al.* (2025a). In this model, flexible workload is interpreted as delayed processing, rather than reduced or curtailed demand. Therefore, the entire flexible workload needs to be executed within the allowed delay time, maintaining the overall computation work.

Electricity can be supplied by the utility grid, on-site photovoltaic generation, wind generation, battery discharge, and UPS discharge. Photovoltaic and wind generation are treated as time-varying renewable sources whose output depends on solar radiation, temperature, and wind speed. The optimization model determines how the available renewable electricity, grid electricity, battery storage, and UPS are used at each step while maintaining the required power balance.

The operational problem is to coordinate flexible workload scheduling, renewable generation, battery operation, UPS operation and grid electricity while satisfying the system constraints. Flexible demand can be shifted to other hours within the delay window allowed. The battery and UPS can be charged or discharged within their operational limits. This enables the model to analyze the potential of these flexibility options to reduce grid electricity consumption and improve the utilization of available renewable generation. Representing workload flexibility as a scarce and time-dependent resource is consistent with Takcı *et al.* (2025b).

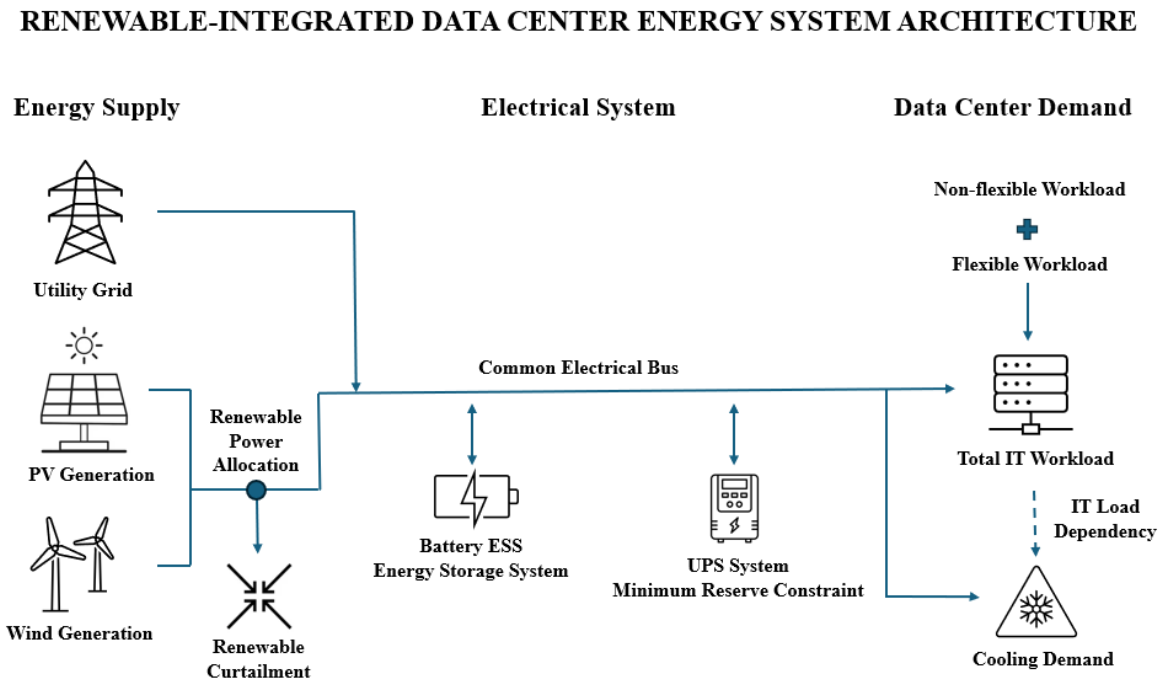

Figure 3.1. Schematic representation of power flows within the renewable-integrated data center system.

As illustrated in Figure 3.1, electricity is supplied by the utility grid, photovoltaic generation, and wind generation through a common electrical bus. Unused renewable power is curtailed, while the available renewable electricity may be allocated to the data-center load, battery storage, or the UPS. The battery energy storage system (ESS) can be charged/discharged within the range of operation. UPS is also allowed to charge or discharge subject to its energy capacity, power limits, efficiency and minimum reserve requirement. A backup generator is not included in the simulation because this thesis focuses on renewable energy integration and energy management during normal grid-connected operation.

On the demand side, the non-flexible and flexible workload components form the total IT workload. The cooling system is supplied from the common electrical bus, while its electricity demand depends on the total IT workload, as indicated by the dashed connection. The hourly operation of renewable generation, grid supply, storage systems, workload scheduling, and cooling demand is coordinated through the optimization model.

3.4 Mathematical formulation

This section develops the mathematical representation of the proposed renewable-integrated data center energy management model. The formulation includes photovoltaic generation, wind generation, IT workload power consumption, workload flexibility, battery energy storage, UPS operation, cooling power consumption, and the overall power balance equation. All power terms used in the power balance equation are expressed in kilowatts (kW). The component equations presented in this section are mainly based on formulations available in the literature. Where the final simulation requires an implementation-specific adjustment or additional constraint, this is stated separately without changing the original literature-based formulation.

3.4.1 Photovoltaic power generation model

The photovoltaic output power, denoted by $P_{t,\theta}^{PV}(sor_{t,\theta})$ is calculated based on solar radiation $(sor_{t,\theta})$, ambient temperature AT_t, PV cell temperature $T_{C_{t,\theta}}$, PV current $I_{t,\theta}^{PV}$, PV voltage $V_{t,\theta}^{PV}$, and the module fill factor (FF), following SoltaniNejad Farsangi *et al.* (2018). The corresponding equations are given below:

$$T_{C_{t,\theta}} = AT_t + sor_{t,\theta} \times \left(\frac{N_{OT} - 20}{0.8}\right) \qquad \forall t, \theta \tag{3.1}$$

$$I_{t,\theta}^{PV} = sor_{t,\theta} \times \left[I_{SC} + K_i \times \left(T_{C_{t,\theta}} - 25\right)\right] \quad \forall t, \theta \tag{3.2}$$

$$V_{t,\theta}^{PV} = V_{OC} - K_v \times T_{C_{t,\theta}} \qquad \forall t, \theta \tag{3.3}$$

$$P_{t,\theta}^{PV}(sor_{t,\theta}) = N^{PV} \times FF \times V_{t,\theta}^{PV} \times I_{t,\theta}^{PV} \qquad \forall t, \theta \tag{3.4}$$

$$FF = \frac{V_{MPP} \times I_{MPP}}{V_{OC} \times I_{SC}} \tag{3.5}$$

Where,

- $P_{t,\theta}^{PV}(sor_{t,\theta})$ is the PV power output at time t under scenario θ (in kilowatts, kW), as a function of solar radiation,
- $T_{C_{t,\theta}}$ is the PV cell temperature at time t under scenario θ, expressed in degrees Celsius (°C),

- AT_t is the ambient temperature at time t, expressed in degrees Celsius (°C),
- $sor_{t,\theta}$ is the solar irradiance at time t under scenario θ, expressed in kilowatts per square meter (kW/m^2),
- N_{OT} is the nominal operating temperature of the PV module, expressed in degrees Celsius (°C),
- 0.8 represents the reference solar irradiance used in the NOT temperature model, measured in kilowatts per square meter (kW/m^2),
- $I_{t,\theta}^{PV}$ is the PV output current at time t under scenario θ, measured in amperes (A),
- I_{SC} is the short-circuit current of the PV module, expressed in amperes (A),
- $K_i$is the temperature coefficient of PV current, measured in amperes per degree Celsius (A/°C),
- 25 means the reference PV cell temperature under Standard Test Conditions (STC),
- $V_{t,\theta}^{PV}$ is the PV output voltage at time t under scenario θ, measured in volts (V),
- V_{OC} is the open-circuit voltage of the PV module, measured in volts (V),
- K_v is the temperature coefficient of PV voltage, measured in volts per degree Celsius ($V/°C$),
- N^{PV} is the number of PV modules and is dimensionless,
- FF is the PV module fill factor and is dimensionless,
- V_{MPP} is the voltage at the maximum power point, measured in volts (V),
- I_{MPP} is the current at the maximum power point, measured in amperes (A),
- t is the time index, dimensionless,
- θ is the scenario index, dimensionless,
- $\forall t, \theta$ means that the equations are applied for all time periods and all scenarios.

Overall, these equations show that PV power output is primarily determined by solar irradiance, cell temperature, module voltage and current, and the fill factor.

For the implemented PV calculation, the effect of temperature on module voltage is evaluated relative to the reference cell temperature of 25 °C under STC. The temperature deviation is calculated as the difference between the actual cell temperature and this reference value, following established PV modeling practice (Villalva *et al.,* 2009). The manufacturer-specified voltage temperature coefficient of the selected module is then applied to the calculated temperature deviation.

3.4.2 Wind turbine power generation model

Wind-turbine power at time t under scenario θ varies nonlinearly with wind speed. A piecewise representation is used to describe turbine operation across the cut-in, rated and cut-out wind-speed regions. The cut-in speed (V_{ci}), rated speed (V_r) and cut-out speed (V_{co}) determine the corresponding operating range. No power is generated when wind speed is below the cut-in speed or above the cut-out speed (SoltaniNejad Farsangi *et al.,* 2018).

The wind turbine power output $P_{wind}(t,\theta)$ is given by the following piecewise function:

$$P_{t,\theta}^{wind} = \begin{cases} 0 & V_{t,\theta}^{W} \le V_{ci} \\ P_r \times \left(\frac{V_{t,\theta}^{W} - V_{ci}}{V_r - V_{CO}}\right)^3 & V_{ci} \le V_{t,\theta}^{W} \le V_r \\ P_r & V_r \le V_{t,\theta}^{W} \le V_{co} \\ 0 & V_{t,\theta}^{W} \ge V_{co} \end{cases} \qquad \forall\, t,\theta \qquad (3.6)$$

Where,

- $P_{t,\theta}^{wind}$ is the wind-turbine power output at time t and scenario θ (in kilowatts, kW),
- $V_{t,\theta}^{W}$ is the wind speed at time t and scenario θ (in meters per second, m/s),
- V_{ci} is the cut-in wind speed (m/s), this is the minimum wind speed required for the turbine to start generating power,
- V_r is the rated wind speed (m/s), the wind speed at which the turbine generates maximum rated power,
- V_{co} is the cut-out wind speed (m/s), above this speed, the turbine stops generating power for safety reasons,

- P_r is the rated power of the wind turbine, this is the maximum power the turbine can produce (in kilowatts, kW),
- t is the time index,
- θ is the scenario index. It represents uncertainty cases, such as different wind speed scenarios.
- W is the superscript indicating wind. It separates the wind speed from other possible speeds or variables.

The equation represents wind-turbine power generation across the cut-in, rated-power, and cut-out operating regions.

3.4.3 IT workload flexibility equation

The relationship between central processing unit (CPU) utilization and IT power consumption is commonly used in detailed data center workload modeling. In this thesis, this relationship is presented as a reference formulation for IT workload power behavior, based on Takcı *et al.* (2025b).

The power consumption of an IT task at any given time t is described as,

$$P_t^{IT} = P_{idle}^{IT} + (P_{max}^{IT} - P_{idle}^{IT}) \times u_t^{1.32} \tag{3.7}$$

Where,

- P_t^{IT} is the IT equipment power demand at time t, expressed in kilowatts (kW);
- P_{idle}^{IT} is the power consumed by the IT equipment when CPU utilization is zero or the equipment is in an idle state, expressed in kilowatts (kW),
- P_{max}^{IT} is the maximum IT equipment power demand at full CPU utilization, expressed in kilowatts (kW),
- u_t is the CPU utilization fraction at time t and is dimensionless,
- The exponent 1.32 is an empirical parameter used to represent the nonlinear relationship between CPU utilization and IT power consumption.

The CPU-utilization equation is retained as a literature-based reference formulation from Takcı *et al.* (2025b). However, CPU utilization is not used directly to calculate the hourly IT power in the final simulation. Instead, the simulation uses time-varying flexible and non-flexible workload profiles. Non-flexible workload is processed when it arrives, while flexible workload can be rescheduled within the allowed delay window. The resulting total IT power is constrained by the installed IT capacity.

3.4.4 IT workload scheduling and demand preservation

Workload shifting in this thesis is based on the idea that flexible IT workloads can be rescheduled in time, but they cannot be removed from the total computational demand. This approach is consistent with the data center flexibility and workload scheduling concepts discussed by Takcı *et al.* (2025a) and Takcı *et al.* (2025b). Therefore, flexible workload shifting does not reduce the total amount of computation to be performed; instead, it shifts the timing of electricity consumption.

The IT workload in the operational simulation changes over time according to the predefined flexible and non-flexible workload profiles. The non-flexible workload must be processed in the hour in which it arrives, whereas the flexible workload may be shifted within the allowable delay window. The total scheduled IT power is constrained by the installed IT capacity.

The demand-preservation requirement is represented by ensuring that all flexible workload arriving during the simulation horizon is scheduled within its allowable delay window. In other words, flexible workload is deferred only temporarily and must still be completed. This keeps the total computational work unchanged while allowing part of the IT demand to be shifted to other hours when this improves the optimized system operation.

When workload shifting is disabled, flexible workload cannot be deferred and must be processed in the hour in which it arrives.

3.4.5 Battery storage system

The battery-storage formulation is adapted from Seyfi *et al.* (2022). The energy stored in the battery at time t depends on its stored energy in the previous time step, the charging and discharging power, the battery efficiency, and the cycling-loss coefficient. The charging and discharging powers are constrained by the battery's energy and power limits. The battery energy-balance equation is expressed as follows:

$$E_t^{ESS} = (1 - Loss^{ESS}) \times E_{t-1}^{ESS} + \left(\eta^{ESS} \times p_{ch,t}^{ESS}\right) - \left(\frac{p_{dch,t}^{ESS}}{\eta^{ESS}}\right) \tag{3.8}$$

For a general time-step duration Δt,, the equation can be written as follows:

$$E_t^{ESS} = (1 - Loss^{ESS}) \times E_{t-1}^{ESS} + \left(\eta^{ESS} \times p_{ch,t}^{ESS} \times \Delta t\right) - \left(\frac{p_{dch,t}^{ESS} \times \Delta t}{\eta^{ESS}}\right) \tag{3.9}$$

Where,

- E_t^{ESS} is the energy stored in the battery at time t (in kilowatt-hours, kWh),
- $Loss^{ESS}$ is the fractional battery cycling-loss coefficient and is dimensionless,
- η^{ESS} is the battery efficiency coefficient and is dimensionless,
- $p_{ch,t}^{ESS}$ is the battery charging power at time t, expressed in kilowatts (kW),
- $p_{dch,t}^{ESS}$ is battery discharging power at time t, expressed in kilowatts (kW),
- Δt is the simulation time-step duration, equal to 1 hour in this study.

Although the literature-based formulation includes the battery loss coefficient in the stored-energy equation, the implemented simulation treats this coefficient as an additional cycling loss associated with charging and discharging. It is not applied as continuous self-discharge when the battery is idle. This prevents unnecessary depletion of stored energy during periods when the battery is not operating, while retaining the charging and discharging efficiencies and battery energy limits.

The battery storage system constraints are as follows:

$$Cap^{ESS,min} \leq E_t^{ESS} \leq Cap^{ESS,max} \tag{3.10}$$

$$0 \leq p_{ch,t}^{ESS} \leq p_{ch}^{ESS,max} \tag{3.11}$$

$$0 \leq p_{dch,t}^{ESS} \leq p_{dch}^{ESS,max} \tag{3.12}$$

Where,

- $Cap^{ESS,min}$ is the minimum allowable energy stored in the battery, expressed in kilowatt-hours (kWh),
- $Cap^{ESS,max}$ is the maximum allowable energy stored in the battery, expressed in kilowatt-hours (kWh),
- $p_{ch}^{ESS,max}$ is the maximum permitted battery charging power, expressed in kilowatts (kW),
- $p_{dch}^{ESS,max}$ is the maximum permitted battery discharging power, expressed in kilowatts (kW).

In the final operational optimization, the literature-based battery formulation is adapted to distinguish between renewable-to-battery and grid-to-battery charging. The total battery charging power is therefore expressed as:

$$P_{B,ch,t} = P_{ren \to B,t} + P_{grid \to B,t} \tag{3.13}$$

Where, $P_{ren \to B,t}$ and $P_{grid \to B,t}$ represent renewable-to-battery and grid-to-battery charging power, respectively.

represent renewable-to-battery and grid-to-battery charging power, respectively.

$$E_{B,t+1} = E_{B,t} + \eta_{B,ch}(1 - Loss_B)P_{B,ch,t}\Delta t - \frac{P_{B,dis,t}\Delta t}{\eta_{B,dis}(1 - Loss_B)} \tag{3.14}$$

Here, $E_{B,t}$ is the operational battery energy, $\eta_{B,ch}$ and $\eta_{B,dis}$ are the charging and discharging efficiencies, $P_{B,dis,t}$ is the battery discharging power, and $Loss_B$ is the cycling-loss coefficient used in the operational model. The loss coefficient is applied during battery charging and discharging rather than as continuous hourly self-discharge.

The battery remains subject to the energy-capacity and charging and discharging power limits presented above. The additional binary operating-mode constraints and the initial and terminal battery-energy conditions are presented in Section 3.6.2.

3.4.6 UPS energy and net power formulation

The UPS formulation is adapted from Takcı *et al.* (2025b). UPS operation is represented through its stored energy, charging and discharging power, energy limits, and net power

exchange with the data center energy system. The UPS stored energy changes according to the charging and discharging powers and their corresponding efficiencies, while remaining within its defined energy and power limits.

The stored energy of UPS is updated at each time step according to the charging and discharging powers and their corresponding efficiencies:

$$E_{t+\Delta t}^{UPS} = E_t^{UPS} + \left(\eta_{ch}^{UPS} \cdot P_{ch,t}^{UPS} \cdot \Delta t\right) - \left(\frac{P_{disch,t}^{UPS}}{\eta_{disch}^{UPS}} \cdot \Delta t\right), \forall t \in T^{ext} \quad (3.15)$$

$$E_{min}^{UPS} \leq E_t^{UPS} \leq E_{max}^{UPS}, \quad \forall t \in T^{ext} \quad (3.16)$$

$$E_{min}^{UPS} = SoC_{min} \cdot E_{base}^{UPS}, \quad E_{max}^{UPS} = SoC_{max} \cdot E_{base}^{UPS} \quad (3.17)$$

$$E_{start}^{UPS} = E_{end}^{UPS} = (50\%) \cdot E_{base}^{UPS} \quad (3.18)$$

$$z_{ch,t}^{UPS} \cdot P_{ch,min}^{UPS} \leq P_{ch,t}^{UPS} \leq z_{ch,t}^{UPS} \cdot P_{ch,max}^{UPS}, \quad \forall t \in T^{ext} \quad (3.19)$$

$$z_{disch,t}^{UPS} \cdot P_{disch,min}^{UPS} \leq P_{disch,t}^{UPS} \leq z_{disch,t}^{UPS} \cdot P_{disch,max}^{UPS}, \quad \forall t \in T^{ext} \quad (3.20)$$

$$z_{ch,t}^{UPS} + z_{disch,t}^{UPS} \leq 1, \quad \forall t \in T^{ext} \quad (3.21)$$

$$P_{net,t}^{UPS} = P_{ch,t}^{UPS} - P_{disch,t}^{UPS}, \quad \forall t \in T^{ext} \quad (3.22)$$

Where,

- E_t^{UPS} is the energy stored in the UPS at time t, usually measured in kilowatt-hours (kWh),
- $E_{t+\Delta t}^{UPS}$ is the UPS stored energy at the end of the next interval, after charging or discharging, measured in (kWh),
- Δt is the duration of one simulation time step, usually measured in hours (h),
- η_{ch}^{UPS} is the UPS charging efficiency and is dimensionless,
- η_{disch}^{UPS} is the UPS discharging efficiency and is dimensionless,
- $P_{ch,t}^{UPS}$ is the UPS charging power at time t measured in kilowatts (kW),
- $P_{disch,t}^{UPS}$ is the UPS discharging power at time t measured in kilowatts (kW),
- E_{min}^{UPS} is the minimum allowable UPS stored energy, measured in kilowatt-hours (kWh), represents the required reserve level.
- E_{max}^{UPS} is the maximum allowable UPS stored energy, measured in kilowatt-hours (kWh), represents the maximum reserve level.

- SoC_{min} is the minimum allowable UPS state of charge, expressed as a dimensionless fraction or percentage.
- SoC_{max} is the maximum allowable UPS state of charge, expressed as a dimensionless fraction or percentage.
- E_{base}^{UPS} is the rated energy capacity of the UPS, which is measured in kilowatt-hours (kWh).
- E_{start}^{UPS} is the energy stored in the UPS at the beginning of the optimization period, which is measured in kilowatt-hours (kWh).
- E_{end}^{UPS} is the stored energy of the UPS at the end of the optimization period, which is measured in kilowatt-hours (kWh).
- 50% means the UPS is assumed to begin and end the optimization period at 50% of its rated energy capacity.
- $z_{ch,t}^{UPS}$ is the binary UPS charging-status variable at time t. It is dimensionless and can only be 0 or 1. A value of 1 allows charging, while a value of 0 prevents charging.
- $z_{disch,t}^{UPS}$ is the binary UPS discharging-status variable at time t. It is dimensionless and can only be 0 or 1. If it's 1, A value of 1 allows discharging, while a value of 0 prevents discharging.
- $P_{ch,min}^{UPS}$ is the minimum allowable UPS charging power, which is measured in kilowatts (kW).
- $P_{ch,max}^{UPS}$ is the maximum allowable UPS charging power, which is measured in kilowatts (kW).
- $P_{disch,min}^{UPS}$ is the minimum allowable UPS discharging power, which is measured in kilowatts (kW).
- $P_{disch,max}^{UPS}$ is the maximum allowable UPS discharging power, which is measured in kilowatts (kW).
- $P_{net,t}^{UPS}$ is the net UPS power exchange at time t, which is measured in kilowatts (kW). It is defined as charging power minus discharging power.

- t is the time index.
- T^{ext} is the extended time horizon used in the optimization model.
- $\forall t \in T^{ext}$ means that the equation is applied for every period t in the extended time horizon.
- UPS as a superscript indicates that the parameter or variable.

These equations describe the literature-based UPS formulation, including its stored-energy balance, energy and power limits, operating-status variables, and net power exchange. In the final operational optimization, the formulation is adapted to distinguish between renewable-to-UPS and grid-to-UPS charging. The total UPS charging power is therefore expressed as:

$$P_{UPS,ch,t} = P_{ren \rightarrow UPS,t} + P_{grid \rightarrow UPS,t} \tag{3.23}$$

Where, $P_{ren \rightarrow UPS,t}$ and $P_{grid \rightarrow UPS,t}$ represent renewable-to-UPS and grid-to-UPS charging power, respectively.

The UPS energy balance used in the operational optimization is:

$$E_{UPS,t+1} = E_{UPS,t} + \eta_{UPS,ch} P_{UPS,ch,t} \Delta t - \frac{P_{UPS,dis,t} \Delta t}{\eta_{UPS,dis}} \tag{3.24}$$

Where, $\eta_{UPS,ch}$ and $\eta_{UPS,dis}$ are the operational charging and discharging efficiencies, respectively.

The UPS stored energy must remain between its minimum reserve and maximum capacity:

$$E_{UPS.reserve} \leq E_{UPS}(t) \leq E_{UPS.max} \tag{3.25}$$

The UPS charging and discharging powers are constrained by:

$$0 \leq P_{UPS,ch,t} \leq P_{UPS,ch}^{max} \tag{3.26}$$

$$0 \leq P_{UPS,dis,t} \leq P_{UPS,dis}^{max} \tag{3.27}$$

The UPS can discharge only the energy stored above its minimum reserve:

$$P_{UPS,dis,t} \leq \frac{(E_{UPS,t} - E_{UPS.reserve}) \eta_{UPS,dis}}{\Delta t} \tag{3.28}$$

This reserve constraint ensures that UPS discharge does not reduce the stored energy below the required minimum level. The additional binary operating-mode constraint and the initial and terminal UPS-energy conditions are presented in Section 3.6.3.

3.4.7 Total cooling power and power-balance formulation

The electricity demand of a data-center cooling system is linked to the IT workload and the corresponding heat-removal requirement. More cooling effort is required to cope with higher IT workload and its associated power consumption in IT equipment. However, cooling demand generally decreases in lower load periods (Zhang *et al.* 2016). In this thesis a simplified operational model is used in which a minimum cooling level is maintained even with the IT load low to represent the basic cooling needed to keep the data center environmental conditions suitable.

Total cooling power is represented as the sum of the main cooling-system components, including rack and server fans, computer room air-handling (CRAH) units, building chilled-water pumps, the chiller, and the cooling tower. Accordingly, the total cooling power is expressed as follows:

$$P_{cooling} = P_{rack_tot} + P_{CRAH_tot} + P_{BCW} + P_{chiller} + P_{CT} \quad (3.29)$$

Where,

- $P_{cooling}$ is the is the total cooling power consumption of the data center, expressed in kilowatts (kW),
- P_{rack_tot} is the total power consumption of the rack and server fans, expressed in kilowatts (kW),
- P_{CRAH_tot} is the total power consumption of the CRAH units, expressed in kilowatts (kW),
- P_{BCW} is the power consumption of the building chilled-water system, expressed in kilowatts (kW),
- $P_{chiller}$ is the power consumption of the chiller, expressed in kilowatts (kW),
- P_{CT} is the power consumption of the cooling tower, expressed in kilowatts (kW),
- $CRAH$ means Computer Room Air Handling unit.
- BCW means Building Chilled Water.
- CT means Cooling Tower.

In the original cooling formulation, cooling demand is represented as a rate of energy consumption and is therefore equivalent to power. In this thesis, the notation, $P_{cooling}$ is adopted for consistency with the overall data-center power-balance formulation. At time t under scenario θ, the cooling power is denoted by $P_{t,\theta}^{cooling}$:

$$P_{t,\theta}^{cooling} = P_{cooling,t,\theta} \quad \forall t, \theta \tag{3.30}$$

Where, $P_{t,\theta}^{cooling}$ is the cooling power included in the data-center power-balance equation at time t under scenario θ, measured in kilowatts (kW).

PUE is a widely used metric for evaluating data-center energy efficiency. It is defined as the ratio of total facility power consumption to IT equipment power consumption and is expressed as follows:

$$PUE = \frac{P_{IT_tot} + P_{cooling} + P_{other}}{P_{IT_tot}} \tag{3.31}$$

Where,

- P_{IT_tot} is the total power consumption of the servers and other IT equipment, expressed in kilowatts (kW),
- P_{other} is the power consumption of other facility components, including lighting and power losses in the UPS and power distribution units (PDUs), expressed in kilowatts (kW),

PUE is dimensionless because all power quantities in Equation (3.31) are expressed in the same unit.

The component-level cooling formulation and PUE expression are included here as the literature-based background for data center cooling and energy use, following Zhang *et al.* (2016). They are not calculated component by component in the final operational simulation. Instead, the simulation represents cooling demand using the aggregated IT-load-dependent cooling formulation presented in the operational constraints.

The IT and cooling power terms together form the main data-center electrical demand. Based on these demand components, the overall power balance requires the total power supplied to the common electrical bus to equal the total power consumed at each time step and under each scenario. The available supply consists of grid electricity, photovoltaic and wind

generation, battery discharge, and UPS discharge. The demand side includes IT workload power, cooling power, battery charging, and UPS charging.

$$P_{t,\theta}^{grid} + P_{t,\theta}^{Pv}(sor_{t,\theta}) + P_{t,\theta}^{wind} + p_{dch,t,\theta}^{ESS} + P_{disch,t,\theta}^{UPS} = P_t^{IT} + P_{t,\theta}^{cooling} + p_{ch,t,\theta}^{ESS} + P_{ch,t,\theta}^{UPS}, \quad \forall t, \theta \tag{3.32}$$

Although the battery and UPS models are originally expressed as time-dependent formulations, they are indexed by scenario θ in the power balance equation to represent their operation under the different simulation scenarios. This equation ensures that the electricity supplied by the grid, renewable energy sources, battery discharge, and UPS discharge is equal to the electricity required by the IT workload, cooling system, battery charging, and UPS charging. All power terms in the equation are expressed in kilowatts (kW).

Grid export is not considered in this study. The photovoltaic and wind terms appearing in the power balance therefore represent the portion of available renewable generation that is utilized within the data center energy system. Renewable electricity may be used directly by the data center load or for charging the battery and UPS. Any available renewable generation that is not utilized during a given time interval is treated as renewable curtailment. The corresponding renewable availability and curtailment constraints are presented later in Section 3.6.

3.5 Operational objective function

The operational objective is to minimize the total electricity imported from the utility grid over the simulation period. The optimization model coordinates renewable generation, battery and UPS operation, and flexible IT workload scheduling subject to the technical and operational constraints of the data center energy system.

For each simulation scenario θ, the objective is formulated as:

$$\min J_\theta = \sum_{t=1}^{T} P_{t,\theta}^{grid} \Delta t \tag{3.33}$$

Where,

- J_θ is total grid electricity imported during the simulation period under scenario θ, measured in kilowatt-hours (kWh),

- $P_{t,\theta}^{grid}$ is the grid-import power at time t under scenario θ, measured in kilowatts (kW),
- T is the number of time steps in the simulation period,
- Δt is the duration of each simulation time step, equal to 1 hour in this study,
- t is the time-step index,
- θ is the scenario index.

Because the simulation uses an hourly time step, multiplying grid power by Δt gives the corresponding grid electricity consumption in kWh. Summing this value over the full simulation horizon gives the total grid electricity imported by the data center.

No separate penalty is applied to renewable curtailment, battery charging, grid-assisted storage charging, flexible workload delay, or UPS discharge in the final objective function. Instead, these decisions are made by the optimization model while satisfying the corresponding technical constraints. For example, flexible workload must still be completed within its allowed delay window, the battery must remain within its energy and power limits, and the UPS must maintain its required minimum energy reserve.

Renewable electricity is therefore used when it helps reduce grid electricity import, while excess renewable generation may be curtailed when it cannot be effectively used within the system constraints. Similarly, battery and UPS charging and discharging are determined by the optimizer rather than by predefined deficit-hour or emergency-only operating rules. Grid charging of the storage systems is also allowed within their respective operating constraints.

Using the same objective function for all scenarios allows their performance to be compared consistently. Differences in grid electricity consumption therefore result from changes in renewable capacity, battery capacity, and workload flexibility rather than from changes in the optimization objective.

3.6 Operational constraints

The objective function seeks to minimize total grid electricity imports, whereas the operational constraints specify the permissible operation of the data center energy system.

These constraints ensure power balance, renewable energy availability, battery and UPS operating limits, IT workload scheduling, IT capacity limits, and cooling demand.

In the final optimization model, battery operation, UPS operation, grid-assisted charging, renewable energy allocation, and flexible workload scheduling are determined directly by the optimizer. No predefined renewable-deficit or non-deficit indicators are used to control these decisions.

3.6.1 Renewable generation and power balance

At each time step t and scenario θ, the total available renewable power is obtained from PV and wind generation:

$$P_{ren,t,\theta} = P_{PV,t,\theta} + P_{WT,t,\theta} \tag{3.34}$$

Where, $P_{PV,t,\theta}$ and $P_{WT,t,\theta}$ denote the available photovoltaic and wind-power generation profiles, respectively. These profiles are model inputs rather than decision variables.

The available renewable power may be supplied directly to the data-center load, allocated to battery or UPS charging, or curtailed:

$$P_{ren,t,\theta} = P_{ren\rightarrow load,t,\theta} + P_{ren\rightarrow B,t,\theta} + P_{ren\rightarrow UPS,t,\theta} + P_{curt,t,\theta} \tag{3.35}$$

The total data-center demand comprises the IT and cooling loads:

$$P_{load,t,\theta} = P^{IT}_{t,\theta} + P_{cool,t,\theta} \tag{3.36}$$

The power supplied to the data center load must satisfy:

$$P_{ren\rightarrow load,t,\theta} + P_{grid\rightarrow load,t,\theta} + P_{B,dis,t,\theta} + P_{UPS,dis,t,\theta} = P_{load,t,\theta} \tag{3.37}$$

The total grid import is defined as:

$$P_{grid,t,\theta} = P_{grid\rightarrow load,t,\theta} + P_{grid\rightarrow B,t,\theta} + P_{grid\rightarrow UPS,t,\theta} \tag{3.38}$$

All power-flow variables are non-negative, and grid export is not considered. Renewable curtailment is not directly penalized in the objective function. Instead, the optimizer minimizes total grid electricity import while deciding how available renewable power, grid electricity, battery storage, and UPS capacity are used within their operating constraints. The battery and UPS charging relationships are defined in Sections 3.6.2 and 3.6.3.

3.6.2 Battery constraints

In addition to the battery energy-balance, energy-capacity, and charging and discharging power constraints presented in Section 3.4.5, the operational optimization includes a binary operating-mode variable to prevent simultaneous battery charging and discharging.

A binary operating-mode variable $u_B(t)$ is introduced to ensure that the battery cannot charge and discharge simultaneously:

$$u_{B,t} \in \{0,1\} \tag{3.39}$$

$$P_{B,ch,t} \leq u_{B,t} P_{B,ch}^{max} \tag{3.40}$$

$$P_{B,dis,t} \leq (1 - u_{B,t}) P_{B,dis}^{max} \tag{3.41}$$

When $u_{B,t} = 1$, battery charging is permitted and discharging is prevented. When $u_{B,t} = 0$, battery discharging is permitted and charging is prevented. These constraints ensure that the battery cannot charge and discharge during the same time step.

The initial battery energy is specified as:

$$E_{B,1} = E_B^{initial} \tag{3.42}$$

and the battery is required to return to the same energy level at the end of the simulation:

$$E_{B,T+1} = E_B^{initial} \tag{3.43}$$

The terminal-energy constraint prevents the optimizer from reducing grid electricity imports by depleting the battery before the end of the simulation. Battery charging and discharging are not restricted to predefined renewable-surplus, renewable-deficit, or other predetermined operating periods. Instead, the optimizer determines battery operation while minimizing total grid electricity import and satisfying the battery constraints presented in Section 3.4.5.

3.6.3 UPS constraints

In addition to the UPS energy-balance, reserve, capacity, charging and discharging power constraints presented in Section 3.4.6, the operational optimization uses a binary operating-mode variable to prevent simultaneous UPS charging and discharging.

A binary operating-mode variable $u_{UPS}(t)$ is introduced to ensure that the UPS cannot charge and discharge simultaneously:

$$u_{UPS,t} \in \{0,1\} \tag{3.44}$$

$$P_{UPS,ch,t} \leq u_{UPS,t} P_{UPS,ch}^{max} \tag{3.45}$$

$$P_{UPS,dis,t} \leq (1 - u_{UPS,t}) P_{UPS,dis}^{max} \tag{3.46}$$

When $u_{UPS,t} = 1$ UPS charging is permitted and discharging is prevented. When $u_{UPS,t} = 0$, UPS discharging is permitted and charging is prevented. These constraints ensure that the UPS cannot charge and discharge during the same time step.

The initial UPS energy is specified as:

$$E_{UPS,1} = E_{UPS}^{initial} \tag{3.47}$$

and the UPS is required to return to the same energy level at the end of the simulation:

$$E_{UPS,T+1} = E_{UPS}^{initial} \tag{3.48}$$

The terminal-energy constraint prevents the optimizer from reducing grid electricity imports by depleting the UPS before the end of the simulation. UPS charging and discharging are not restricted to predefined renewable surplus, renewable-deficit, or other predetermined operating periods. Instead, the optimizer determines UPS operation while minimizing total grid electricity import and maintaining the required minimum stored-energy reserve.

3.6.4 IT workload shifting constraints

The IT load consists of non-flexible and flexible workload:

$$P_t^{IT} = P_{nonflex,t} + P_{flex,sch,t} \tag{3.49}$$

The non-flexible workload must be processed in the hour in which it arrives:

$$P_{nonflex,t} = P_{nonflex,arrival,t} \tag{3.50}$$

Let, $x_{s,t}$ represent the amount of flexible workload that arrives at hour s and is processed at hour t. Each flexible workload arrival must be completed within the maximum delay D_{max}:

$$\sum_{t=s}^{\min(T,s+D_{max})} x_{s,t} = P_{flex,arrival,s} \Delta t \tag{3.51}$$

With

$$x_{s,t} \geq 0 \tag{3.52}$$

The scheduled flexible workload at hour t is:

$$P_{flex,sch,t} = \frac{1}{\Delta t} \sum_{s=\max(1,t-D_{max})}^{t} x_{s,t} \quad (3.53)$$

The total IT power must remain within the installed IT capacity:

$$0 \leq P_t^{IT} \leq P_{IT}^{max} \quad (3.54)$$

Where P_{IT}^{max} denotes the installed IT-capacity limit.

The optimizer determines when flexible workload is processed while minimizing total grid electricity import. No predefined renewable-deficit or peak-hour rule is used for workload scheduling. All flexible workload must still be completed within its allowable delay window. In the base optimized scenarios, $D_{max} = 3\ hours$, while $D_{max} = 0$ represents the no-workload-shifting scenario.

3.6.5 Cooling demand constraints

Cooling demand is linked to the IT load because higher IT power consumption produces more heat that must be removed. A minimum cooling level is also maintained during operation:

$$P_{cool,t} = P_{cool,min} + k_{cool} P_t^{IT} \quad (3.55)$$

Where, $P_{cool,min}$ is the minimum cooling demand and k_{cool} is the cooling coefficient.

This formulation makes cooling demand increase directly with the scheduled IT load. Cooling is not treated as a flexible decision variable in the optimization; instead, its value is determined by the IT workload at each time step. The numerical values of the cooling parameters used in the simulation are presented in Chapter 4.

4 Simulation setup and scenario design

4.1 Simulation environment and time horizon

The analysis builds on the component models and assumptions introduced in Chapter 3, including renewable generation, IT workload flexibility, battery storage, UPS operation, and cooling demand. The simulation aims to assess the interaction of the above components in a grid-connected data center, under different conditions of renewables, storage and workload-flexibility.

The simulation is carried out for the year 2025 using an hourly time resolution, resulting in 8760 time steps. At each hour, the optimization model determines grid electricity import, renewable power allocation, battery and UPS charging and discharging, renewable curtailment, and flexible workload scheduling while satisfying the operational constraints defined in Chapter 3.

The optimization model is implemented in Python using Pyomo and solved with the COIN-OR Branch and Cut (CBC) solver. It is formulated as a mixed-integer linear programming (MILP) model that minimizes total grid electricity imports over the simulation period.

The main simulation inputs include hourly solar radiation, ambient temperature, wind speed, flexible and non-flexible IT workload profiles, cooling parameters, battery parameters, and UPS operating limits. PV and wind generation are calculated from meteorological data before being provided to the optimization model as hourly renewable generation profiles.

The IT workload is represented by time-varying flexible and non-flexible hourly profiles rather than by a constant demand. Non-flexible workload must be processed when it arrives, while flexible workload can be shifted within the allowed delay window. The total scheduled IT power is limited by the installed IT-capacity constraint. Cooling demand is calculated from the scheduled IT load using the aggregated cooling model described in Chapter 3.

Both the battery and the UPS are modeled as controllable storage resources. Both the battery and the UPS are modeled as controllable storage resources. The battery may be charged using renewable or grid electricity and is operated within its energy and power limits. The UPS may also charge and discharge according to the optimization decision while

maintaining its minimum energy reserve. The final model uses no predefined renewable-deficit hours, emergency-only UPS rules, or separate penalties for storage operation.

4.2 Simulation scenario design

Six scenarios are simulated using the same optimization model and objective function. The scenarios vary renewable generation, battery capacity, and workload flexibility to examine how these changes affect grid electricity consumption, renewable utilization, and system scalability.

Table 4.1. Scenario settings used for integrated optimization analysis.

Scenario	Setting	Purpose
Base optimized operation	PV 1500 kW, wind 1500 kW, battery 1200 kWh, maximum delay 3 h	Reference optimized case
Low renewable	PV and wind generation × 0.75, battery 1200 kWh, maximum delay 3 h	Examines lower renewable availability
Triple renewable	PV and wind generation × 3, battery 1200 kWh, maximum delay 3 h	Examines renewable capacity scaling
Triple battery	Base renewable generation, battery 3600 kWh, maximum delay 3 h	Examines storage capacity scaling
Triple renewable + triple battery	PV and wind generation × 3, battery 3600 kWh, maximum delay 3 h	Examines combined renewable and storage scaling
Triple renewable, no workload shifting	PV and wind generation × 3, battery 1200 kWh, maximum delay 0 h	Examines the contribution of workload flexibility under high renewable availability

The scenarios in Table 4.1 are not separate mathematical models. The same optimization structure and grid-import-minimization objective are used in all cases, while selected parameters are changed for comparison. Grid-assisted battery and UPS charging remain available in every scenario and are determined by the optimizer.

For the base battery capacity of 1200 kWh, the minimum energy level is 100 kWh and the initial energy is 600 kWh. In the triple-battery scenario, the capacity is increased to 3600 kWh, the minimum energy level is scaled to 300 kWh, and the initial energy is 1800 kWh. The charging and discharging power limits are unchanged. In all cases the battery must be

returned to its initial energy level at the end of the simulation. The UPS capacity is constant for all scenarios at 600 kWh with minimum reserve of 300 kWh. The UPS begins and ends the simulation at 300 kWh.

No fixed dispatch order is imposed on renewable generation, battery storage, UPS operation, or grid electricity. The optimizer determines the hourly power flows while minimizing total grid electricity import and satisfying the system constraints. Grid export is not considered, and any available renewable generation that is not utilized is treated as renewable curtailment.

The scenarios are compared using total grid electricity consumption, renewable generation and utilization, renewable curtailment, battery and UPS operation, and workload shifting. Model-validation checks are also used to confirm that the power balance, renewable allocation, grid definition, and IT capacity constraints are satisfied.

4.3 Renewable energy resource data

Hourly weather observations for 2025 were obtained from the FMI. Kauhajoki Kuja-Kokko was used as the primary weather station, while Kankaanpää Niinisalo airfield was used as a secondary station to fill missing observations. The required variables were wind speed, air temperature, and global solar radiation.

The weather data were aligned to a continuous hourly time series containing 8760 hours. Values from the primary station were used whenever available. Missing values were replaced using observations from the secondary station after applying variable-specific corrections derived from periods where data from both stations were available. For wind speed, an additive correction of +0.1059 m/s was applied to the secondary data, while air temperature was corrected by −0.3129 °C. Secondary solar-radiation values were adjusted using a scaling factor of 1.0428.

After the primary and corrected secondary observations were combined, only short remaining gaps of up to 3 hours were filled by linear interpolation. Negative wind speed and solar-radiation values were set to zero. The final dataset contained 8760 hourly observations with no missing values.

Hourly PV generation was calculated using solar irradiance and ambient-temperature data, whereas hourly wind generation was derived from wind-speed observations. The wind-speed observations were recorded at a height of 10 m, while the selected wind turbine has a hub height of 65 m. Therefore, the observed wind speeds were adjusted to the turbine hub height using the wind-profile power law before the turbine power curve was applied. This approach is commonly used to estimate hub-height wind speeds from measurements collected at lower heights (Jung and Schindler, 2021). A power-law exponent of 0.14 was used as an engineering approximation because site-specific wind data at several heights were not available. However, using a constant exponent introduces uncertainty that should be considered when interpreting the calculated wind generation (Jung and Schindler, 2021). The resulting renewable-generation profiles were used as hourly inputs to the optimization model (FMI n.d.).

Figure 4.1 provides the annual PV generation profile for the base 1500 kW PV installation. The figure shows the hourly variation in PV generation during 2025 resulting from changes in solar irradiance and ambient temperature. This profile serves as the base PV input before renewable-generation scaling is applied in the scenario analysis.

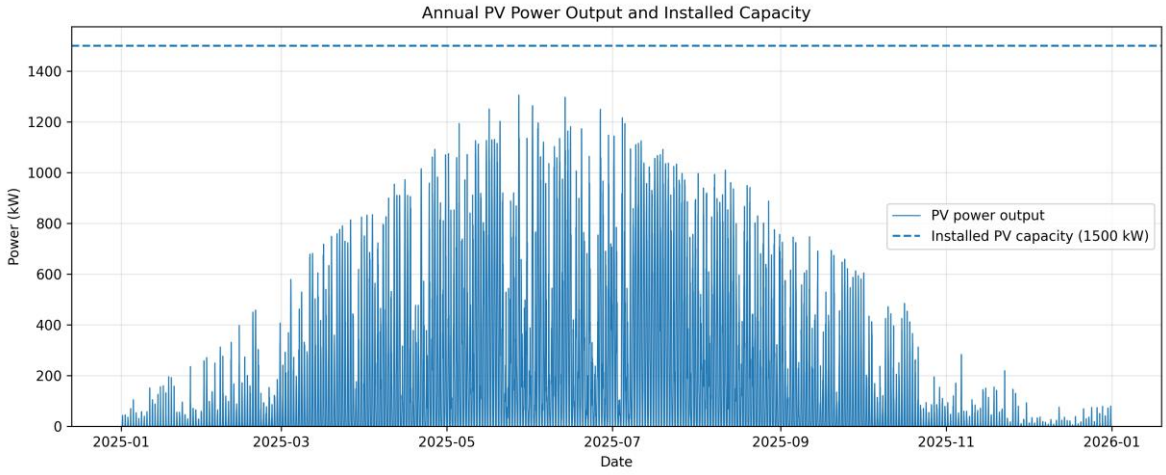

Figure 4.1. Annual photovoltaic generation profile used in the base simulation.

Figure 4.2 presents the corresponding wind-generation profile. Because hourly wind output fluctuates considerably, daily mean and maximum values are shown to make the annual pattern easier to interpret. The original hourly wind-generation values are retained as inputs to the optimization model.

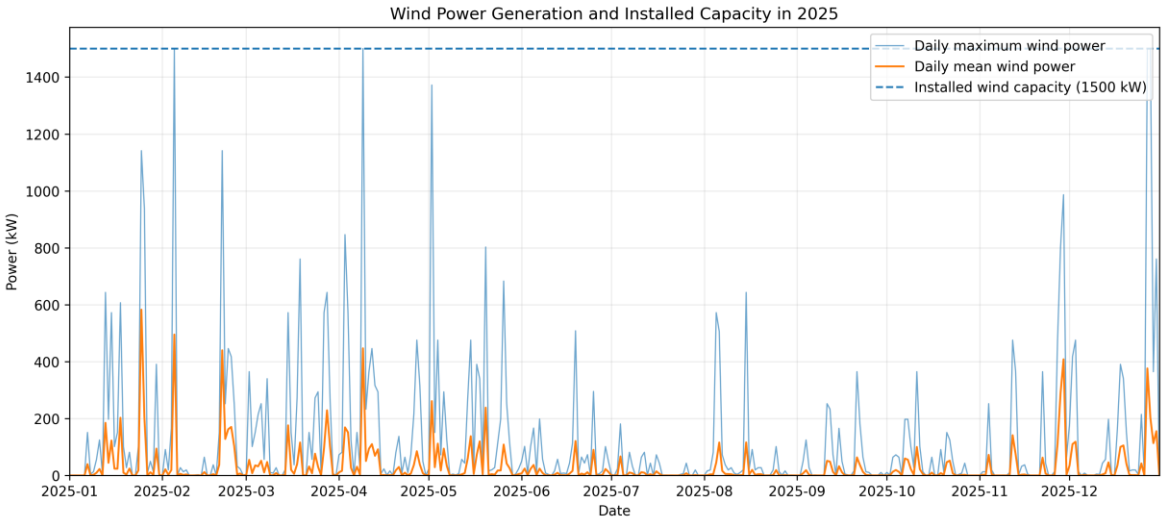

Figure 4.2. Daily mean and maximum wind generation used in the base simulation.

Figures 4.1 and 4.2 therefore represent the base renewable-generation profiles. In the low-renewable and triple-renewable scenarios, these profiles are scaled according to the scenario settings given in Table 4.1.

4.4 Base-case system capacity and component assumptions

The base simulation represents a data center with a defined installed IT-capacity limit. This limit represents the maximum IT power that can be processed at any hour and is not treated as a constant hourly demand. Its numerical value is provided in Table 4.2. The actual IT load varies throughout the simulation according to the flexible and non-flexible workload profiles described earlier.

Cooling demand is time-varying and depends on the scheduled IT workload according to the cooling Equation (3.55) defined in Section 3.6.5. In the simulation, a minimum cooling requirement of 100 kW is adopted together with a cooling coefficient of 0.30. Therefore, the model does not assume a fixed cooling load of 400 kW or a constant total data center demand of 1400 kW.

The base case has a total installed renewable capacity of 3000 kW with 1500 kW installed photovoltaic and 1500 kW installed wind capacity. These capacities are selected as simulation parameters for the renewable-integration and scalability analysis. Hourly

renewable generation varies according to solar irradiance, ambient temperature, and wind speed.

For the PV generation model, the Canadian Solar CS6W-550MB-AG module is adopted as a representative commercial technology. The rated power of the module is 0.55 kW under STC, and the other electrical parameters are taken from the manufacturer datasheet (CSI Solar Co., Ltd., 2024). The model uses a maximum-power-point voltage of 41.70 V, a maximum-power-point current of 13.20 A, an open-circuit voltage of 49.60 V, a short-circuit current of 14.00 A, and a nominal operating cell temperature of 41 °C. Based on the 1500 kW installed PV capacity, 2727 modules are represented in the model. The module is used only to provide the electrical parameters required by the PV model and does not represent a detailed physical design of the PV plant. The PV temperature correction is applied relative to the reference temperature of 25 °C under STC, consistent with the PV modeling approach discussed by Villalva *et al.* (2009).

The wind-generation model uses the GE Vernova GE 1.5s as a representative turbine because its rated capacity corresponds to the 1500 kW wind installation considered in the base case. Its cut-in, rated, and cut-out wind speeds are 4.0 m/s, 13.0 m/s, and 25.0 m/s, respectively (Wind-Turbine-Models.com, 2023).

The FMI wind-speed observations were recorded at a height of 10 m, whereas the selected turbine has a hub height of 65 m. The observed wind speeds are therefore adjusted to hub height using the power-law relationship presented in Chapter 3. This adjustment uses a power-law exponent of 0.14 following the wind-profile approach discussed by Jung and Schindler (2021). The key parameters of the optimized base configuration are summarized below:

Table 4.2. Base-case system and simulation parameters.

Parameter	Base value
Installed IT capacity	1000 kW
Minimum cooling power	100 kW
Cooling coefficient	0.30
Installed PV capacity	1500 kW
Installed wind capacity	1500 kW
Battery capacity	1200 kWh
Maximum workload delay	3 h

These values in Table 4.2 define the base optimized operation. The PV and wind capacities, battery capacity, cooling parameters, and workload-delay limit are simulation parameters used for scenario analysis. The renewable, battery, and workload-flexibility variations used in the other scenarios are presented in Section 4.2.

4.5 IT workload flexibility and computational demand preservation

Table 4.3 presents the workload-flexibility input settings used in the simulation. The maximum deferral window is 3 hours in the workload-shifting scenarios and 0 hours in the no-workload-shifting scenario. The installed IT-capacity limit is specified in Table 4.2.

Table 4.3. IT workload profiles and flexibility settings.

Parameter	Settings	Description
Flexible workload	Time-varying hourly profile	Workload that can be shifted within the allowed delay window
Non-flexible workload	Time-varying hourly profile	Workload that must be processed when it arrives
Simulation time step	1 hour	Hourly optimization interval
Maximum deferral window	3 hours	Maximum delay allowed for flexible workload
No-shifting case	0 hours	Flexible workload must be processed immediately

The simulation preserves the total computational demand by requiring all flexible workload to be completed within its allowable delay window. Therefore, workload shifting changes only the timing of electricity consumption and does not reduce the total amount of computational work.

4.6 Battery storage system specifications

Table 4.4 summarizes the battery parameters adopted for the optimized base case based on Seyfi *et al.* (2022).

Table 4.4. Battery storage energy, power, and efficiency parameters.

Parameter	Value	Description
Charging efficiency, $\eta_{B,ch}$	0.96	Battery charging efficiency
Discharging efficiency, $\eta_{B,dis}$	0.96	Battery discharging efficiency
Battery loss coefficient, $Loss_B$	0.01	Cycling-loss coefficient
Maximum battery capacity, $E_{B,max}$	1200 kWh	Maximum stored energy in the base case
Minimum battery energy, $E_{B,min}$	100 kWh	Minimum allowable stored energy
Initial battery energy	600 kWh	Stored energy at the beginning of the simulation
Maximum charging power, $P_{B,ch}^{max}$	500 kW	Maximum allowable charging power
Maximum discharging power, $P_{B,dis}^{max}$	700 kW	Maximum allowable discharging power
Final battery energy	600 kWh	Required stored energy at the end of the simulation

The battery has a maximum stored-energy capacity of 1200 kWh and a minimum allowable energy level of 100 kWh. This terminal-energy requirement prevents the model from artificially reducing grid electricity imports by depleting the battery at the end of the simulation.

For the triple-battery scenarios, the energy capacity is increased to 3600 kWh. The minimum energy level is scaled to 300 kWh, and the initial and final battery energy levels are set to 1800 kWh, while the charging and discharging power limits remain unchanged.

4.7 UPS characteristics

The UPS parameters adopted in the simulation are presented in Table 4.5. The UPS has a total energy capacity of 600 kWh and must maintain a minimum reserve of 300 kWh. It begins the annual simulation with 300 kWh and is required to return to the same stored-energy level at the end of the optimization period.

Table 4.5. UPS energy, power, efficiency, and operating limits.

Parameter	Value	Description
UPS energy capacity, $E_{UPS.max}$	600 kWh	Maximum stored energy

Minimum UPS reserve, $E_{UPS.reserve}$	300 kWh	Minimum allowable stored energy
Initial UPS energy, $E_{UPS}^{initial}$	300 kWh	Stored energy at the beginning of the simulation
Final UPS energy	300 kWh	Target stored energy at the completion of the simulation
Maximum charging power, $P_{UPS,ch}^{max}$	270 kW	Maximum UPS charging power
Maximum discharging power, $P_{UPS,dis}^{max}$	270 kW	Maximum UPS discharging power
Charging efficiency, $\eta_{UPS,ch}$	0.82	UPS charging efficiency
Discharging efficiency, $\eta_{UPS,dis}$	0.92	UPS discharging efficiency
Charging/discharging status, $u_{UPS,t}$	{0,1}	Binary operating-mode variable that prevents concurrent charging and discharging
Net UPS power, $P_{UPS,net,t}$	$P_{UPS,ch,t} - P_{UPS,dis,t}$	Net power exchange of the UPS

The UPS may be charged from either renewable generation or grid electricity. Its charging and discharging schedule is determined by the optimizer while the stored energy is maintained between 300 and 600 kWh. Since the initial energy is equal to the minimum reserve, the UPS can discharge only after energy has first been stored above the reserve level. Binary operating constraints prevent simultaneous charging and discharging.

4.8 Cooling system specifications

The cooling system is included as a non-IT data center load that must be supplied together with the IT workload. Cooling demand is required because IT equipment produces heat during operation.

The cooling representation follows the data-center cooling framework described by Zhang et al. (2016), in which total cooling power comprises rack and server fans, CRAH units, chilled-water pumps, chillers, and cooling towers. Because these components are not represented individually in this thesis, cooling demand is modeled using the aggregated formulation given in Equation (3.55) in Section 3.6.5. The corresponding parameters are presented in Table 4.6.

Table 4.6. Parameters of the IT-load-dependent cooling model.

Parameter	Value	Description
Minimum cooling power, $P_{cool,min}$	100 kW	Minimum cooling demand used in the model
Cooling coefficient, k_{cool}	0.30	Relates cooling demand to scheduled IT power
Cooling demand at maximum IT capacity	400 kW	Cooling demand when IT power reaches 1000 kW

4.9 Model evaluation criteria

The proposed model is evaluated using performance indicators calculated from the simulation outputs. These indicators are used to compare the operation of the six scenarios and are not included as additional optimization constraints.

The evaluation is based on metrics including grid electricity consumption, renewable energy utilization, renewable curtailment, operation of battery and UPS, workload flexibility and model feasibility. The main indicator for grid dependence is the total grid electricity consumption, which is consistent with the objective function of the optimization model. Effective utilization of available PV and wind generation is evaluated through renewable utilization and curtailment.

Battery and UPS operation is evaluated through their annual charging and discharging behavior and energy limits. Workload flexibility is assessed by comparing the workload-shifting and no-workload-shifting cases while confirming that all computational demand is completed within the allowed delay limits.

Model feasibility is checked through the hourly power balance and other operational constraints. The corresponding maximum errors are calculated to confirm that the optimized solutions satisfy the mathematical constraints.

The combined indicators are then employed to assess the impact of renewable capacity, battery capacity and workload flexibility on the grid electricity dependency, renewable energy utilization, curtailment and overall system operation.

5 Results and discussion

This chapter reports the findings from the annual optimization of the renewable-integrated data center energy management model. Six scenarios are examined to determine how renewable-generation capacity, battery capacity, and workload flexibility influence grid electricity imports and renewable-energy utilization. The analysis also covers renewable curtailment, battery and UPS operation, IT workload scheduling, and model feasibility.

The chapter first compares the overall performance of the six scenarios. It then examines renewable energy utilization and curtailment, followed by the effect of battery capacity and workload flexibility. Representative weekly and 24-hour profiles are presented to demonstrate the operation of the integrated data center energy system. Finally, the optimization outcomes are verified against the main power-balance and operational constraints.

5.1 Overall scenario performance

The overall performance of the six simulation scenarios is compared using annual grid electricity import, renewable generation, renewable energy utilization, and renewable curtailment. Table 5.1 summarizes the main annual results obtained from the optimization model.

Table 5.1. Main annual results of the six simulation scenarios.

Scenario	Grid import (kWh)	Renewable generation (kWh)	Renewable used (kWh)	Renewable utilization (%)	Curtailment (kWh)
Base optimized	5,686,400	1,685,565	1,678,335	99.571	7,230
Low renewable	6,098,673	1,264,174	1,264,126	99.996	48
Triple renewable	4,017,865	5,056,696	3,384,767	66.936	1,671,929
Triple battery	5,680,807	1,685,565	1,684,223	99.920	1,342
Triple renewable + triple battery	3,680,360	5,056,696	3,758,112	74.320	1,298,584
Triple renewable + no workload shifting	4,198,095	5,056,696	3,209,752	63.475	1,846,944

As shown in Table 5.1, the base optimized scenario requires 5,686,400 kWh of grid electricity during the year. Reducing renewable generation to 75% of the base level increases grid import to 6,098,673 kWh. In contrast, increasing renewable generation to three times the base level reduces annual grid import to 4,017,865 kWh.

Increasing only the battery capacity from 1200 kWh to 3600 kWh has very little effect at the base renewable level, reducing grid import from 5,686,400 kWh to 5,680,807 kWh. The lowest grid electricity consumption is achieved when triple renewable generation is combined with the 3600 kWh battery, resulting in 3,680,360 kWh of annual grid import.

Figure 5.1 compares annual grid electricity import across the six scenarios and shows the percentage change relative to the base optimized case.

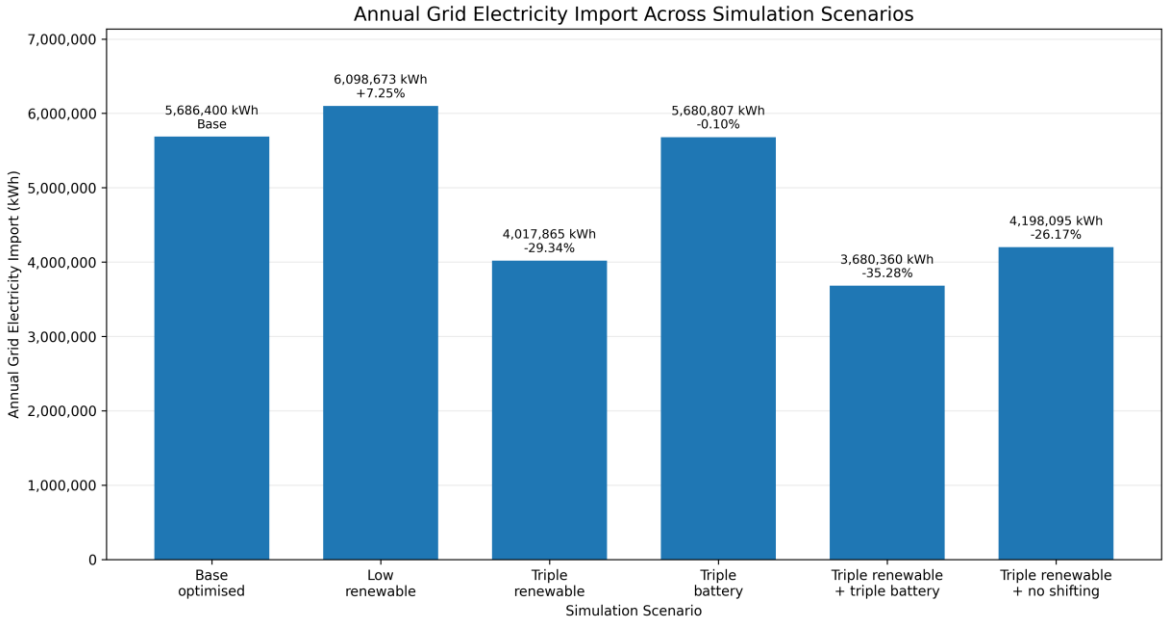

Figure 5.1. Annual grid electricity imports across the six simulation scenarios.

Figure 5.1 indicates that the low-renewable case requires 7.25% more grid electricity than the base case. Triple renewable capacity reduces grid import by 29.34%, while increasing the battery capacity alone produces only a 0.10% reduction. The combined triple-renewable and triple-battery scenario gives the largest reduction, decreasing annual grid import by 35.28% compared with the base optimized case. The triple-renewable scenario without workload shifting still reduces grid import by 26.17% relative to the base case, although its performance is lower than the corresponding case with workload flexibility.

These results show that renewable capacity has a much stronger effect on annual grid dependence than increasing battery capacity alone. However, the benefit of larger storage becomes more noticeable when greater renewable generation is available.

5.2 Renewable utilization and curtailment

Renewable utilization and curtailment show how much of the available PV and wind generation is actually used by the data center energy system. Figure 5.2 compares the renewable utilization rate and annual renewable curtailment across the six simulation scenarios.

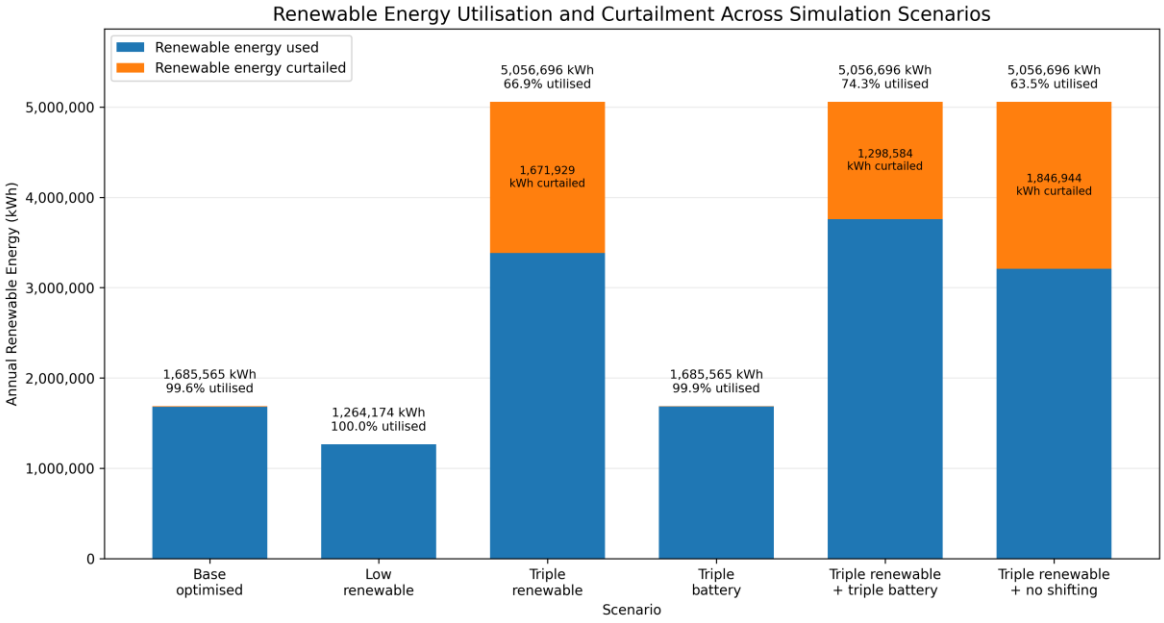

Figure 5.2. Renewable energy utilization and curtailment across the six simulation scenarios.

In the base optimized scenario, 99.57% of the obtainable renewable generation is utilized, only 7,230 kWh is curtailed. The low-renewable scenario has the highest utilization rate (99.996%) because the data center demand and storage system can absorb almost all the available renewable electricity. In this case, the curtailment is only 48 kWh.

When renewable generation is increased to three times the base level, the utilization rate decreases to 66.94%, while annual curtailment increases to 1,671,929 kWh. This indicates that increasing renewable capacity creates periods in which available generation exceeds what can be absorbed under the existing storage and workload-flexibility limits.

Increasing the battery capacity to 3600 kWh has little effect at the base renewable level, where renewable utilization increases only from 99.57% to 99.92%. However, under triple renewable generation, the larger battery increases renewable utilization from 66.94% to 74.32% and reduces curtailment from 1,671,929 kWh to 1,298,584 kWh.

The triple-renewable case without workload shifting has the lowest renewable utilization, at 63.48%, and the highest curtailment, at 1,846,944 kWh. Compared with this case, allowing a 3-hour workload-shifting window increases renewable utilization by about 3.46 percentage points and reduces annual curtailment by approximately 175,015 kWh.

Overall, the results indicate that increasing renewable capacity alone is insufficient to achieve high renewable-energy utilization. Storage capacity and workload flexibility become increasingly important as renewable generation expands.

5.3 Battery capacity and scalability

This section investigates the impact of increasing battery energy capacity on grid electricity import and renewable energy utilization for different renewable generation levels. Figure 5.3 compares the effects of increasing battery energy capacity from 1200 kWh to 3600 kWh under the base-renewable and triple-renewable cases.

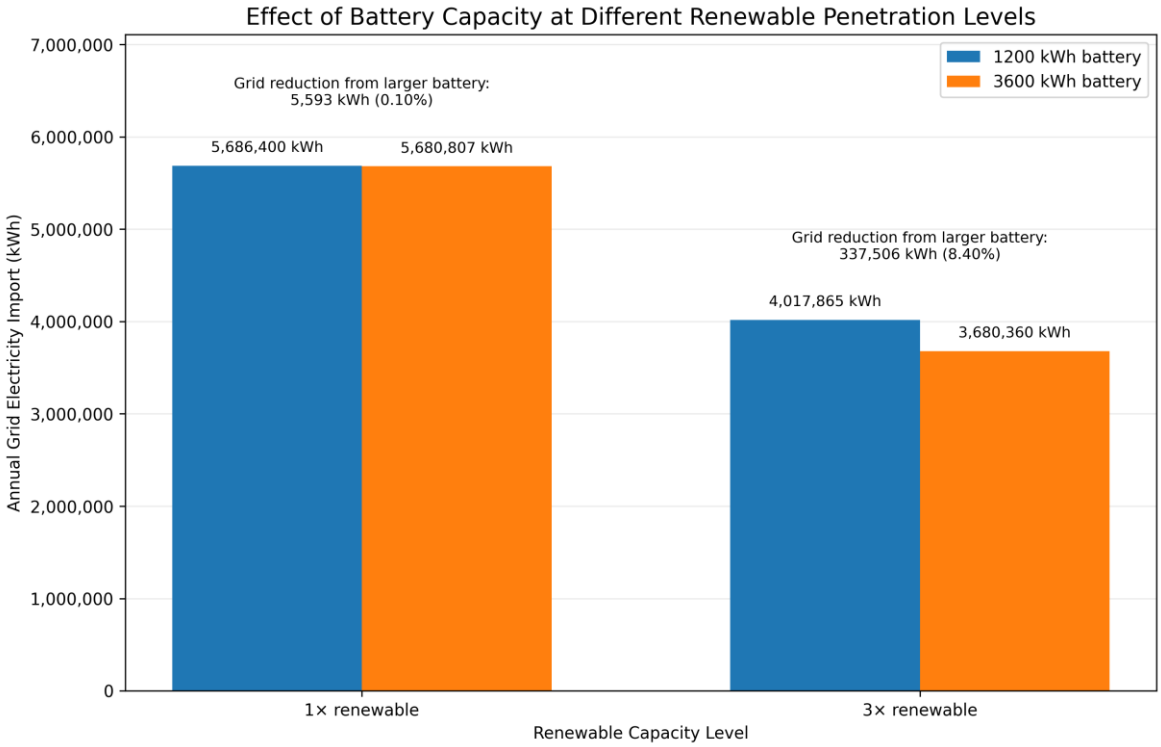

Figure 5.3. Effect of battery capacity on grid electricity import and renewable energy utilization.

At the base renewable level, increasing battery energy capacity from 1200 kWh to 3600 kWh results in only a slight decrease in annual grid electricity imports, from 5,686,400 kWh to 5,680,807 kWh, corresponding to a reduction of approximately 5,593 kWh, or 0.10%. Renewable utilization increases slightly, from 99.57% to 99.92%, while curtailment decreases from 7,230 kWh to 1,342 kWh. This small change is associated with the fact that almost all the available renewable generation is already being used in the base case, and therefore there is little surplus energy for the larger battery to store.

The effect of additional battery capacity is much stronger when renewable generation is tripled. Grid imports decrease from 4,017,865 kWh with the 1200 kWh battery to 3,680,360 kWh with the 3600 kWh battery, corresponding to a reduction of approximately 337,506 kWh, or 8.40%. At the same time, renewable utilization increases from 66.94% to 74.32%, while annual curtailment decreases from 1,671,929 kWh to 1,298,584 kWh.

Battery charging and discharging also increase considerably under the high-renewable condition. In the triple-renewable case, annual battery charging and discharging are approximately 239,727 kWh and 216,536 kWh, respectively. With both triple renewable generation and the 3600 kWh battery, these values increase to approximately 617,759 kWh

and 557,997 kWh, respectively. This shows that the larger battery is used much more actively when sufficient renewable surplus is available. Figure 5.4 presents the daily mean battery state-of-charge profiles for the two battery-capacity cases.

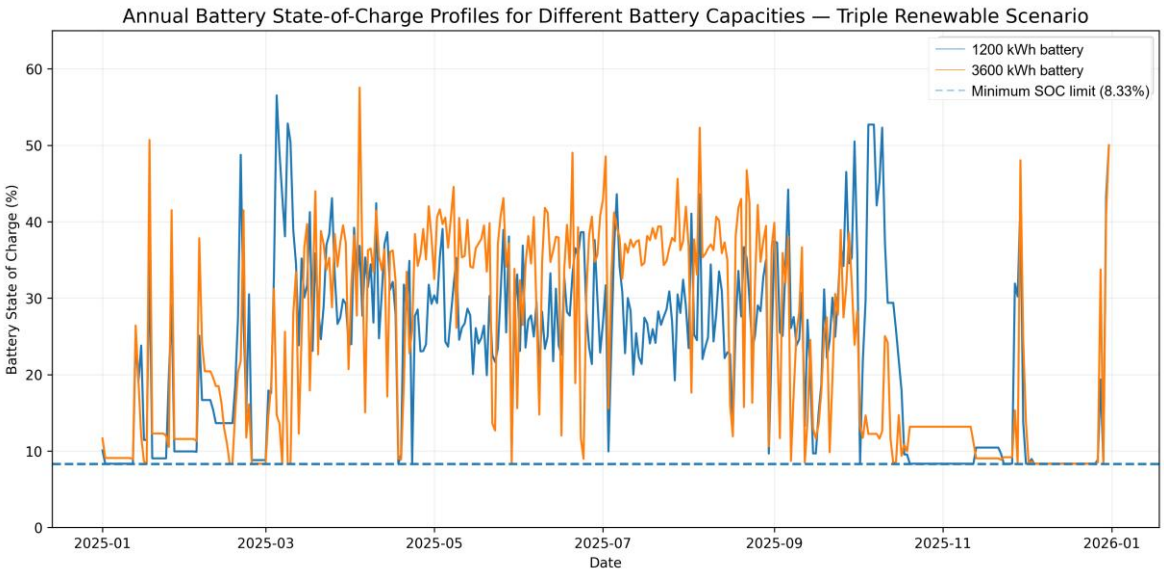

Figure 5.4. Daily mean battery state-of-charge profiles for 1200 kWh and 3600 kWh storage capacities under the triple-renewable scenario.

The 1200 kWh battery has a minimum stored-energy limit of 100 kWh, whereas the 3600 kWh battery uses a proportionally scaled minimum limit of 300 kWh. The initial and final stored-energy levels are 600 kWh for the 1200 kWh battery and 1800 kWh for the 3600 kWh battery. Both battery sizes are required to return to their initial energy level at the end of the annual simulation, ensuring that the comparison is not affected by using stored energy remaining at the start of the simulation.

Overall, the results show that increasing battery capacity alone provides little benefit when renewable surplus is limited. Its value becomes much greater when renewable generation is increased, because the additional storage capacity can absorb more surplus renewable electricity and reduce both curtailment and grid dependence.

5.4 Effect of workload flexibility

The effect of workload flexibility is evaluated by comparing the triple-renewable scenario with a 3-hour workload-shifting window against the triple-renewable scenario with no workload shifting. The renewable capacity, battery capacity, and other system parameters

are the same in both cases, so the difference in performance is caused by workload flexibility. Figure 5.5 compares the monthly grid electricity import and renewable curtailment for the two cases.

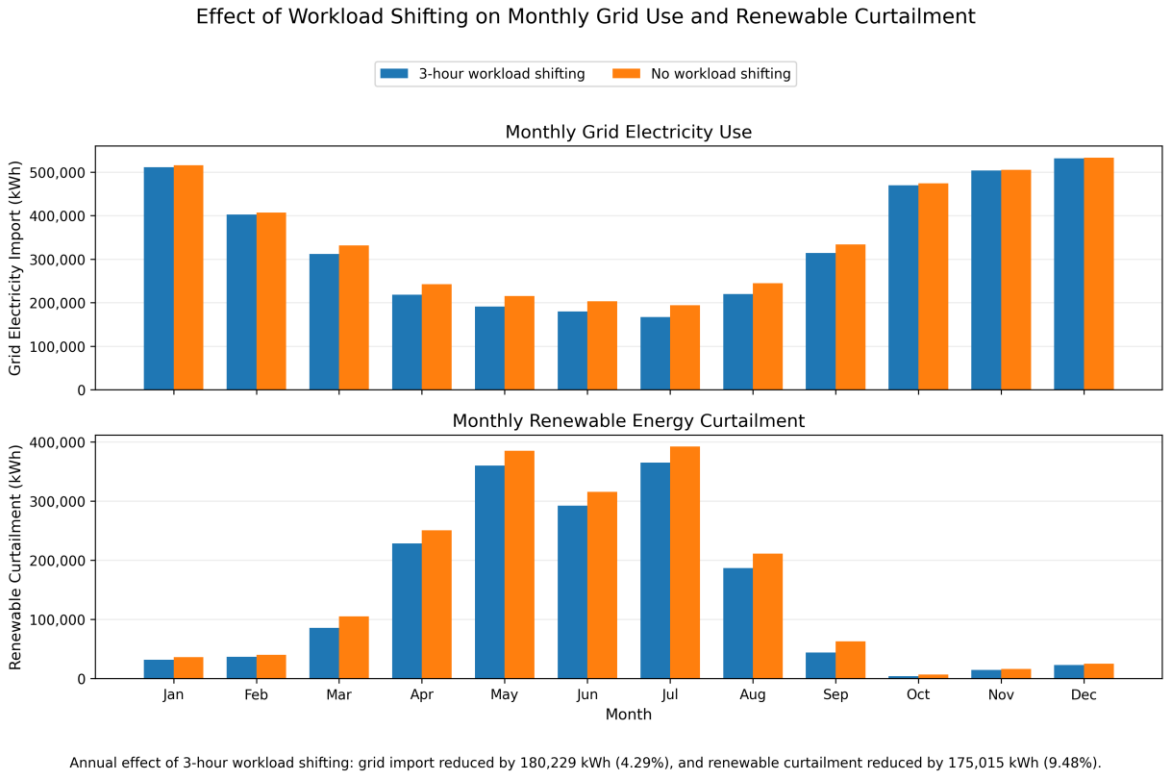

Figure 5.5. Effect of workload shifting on monthly grid electricity import and renewable curtailment.

With 3-hour workload shifting, annual grid electricity import is 4,017,865 kWh, compared with 4,198,095 kWh when workload shifting is disabled. This corresponds to a reduction of approximately 180,229 kWh, or 4.29%.

Workload flexibility also improves renewable-energy utilization. The renewable utilization rate increases from 63.48% without workload shifting to 66.94% with workload shifting, an improvement of about 3.46 percentage points. At the same time, annual renewable curtailment decreases from 1,846,944 kWh to 1,671,929 kWh, corresponding to a reduction of approximately 175,015 kWh, or 9.48%.

As shown in Figure 5.5, the benefit of workload shifting varies over the year and is more visible during periods with higher renewable curtailment. By allowing flexible computing tasks to be delayed by up to 3 hours, the optimizer can move part of the IT demand to more favorable hours without reducing the total computational workload.

Overall, the results show that workload flexibility provides a measurable benefit under high renewable availability by reducing grid electricity consumption and renewable curtailment while improving renewable utilization.

5.5 Representative data-center operation

The annual results show the overall differences between the scenarios, but they do not show how the optimized system behaves from hour to hour. Therefore, representative weekly and 24-hour results are used to illustrate the interaction between IT demand, cooling, renewable generation, storage, and grid electricity. Figure 5.6 shows the optimized data-center electrical demand for 16–22 June 2025 in the base optimized scenario.

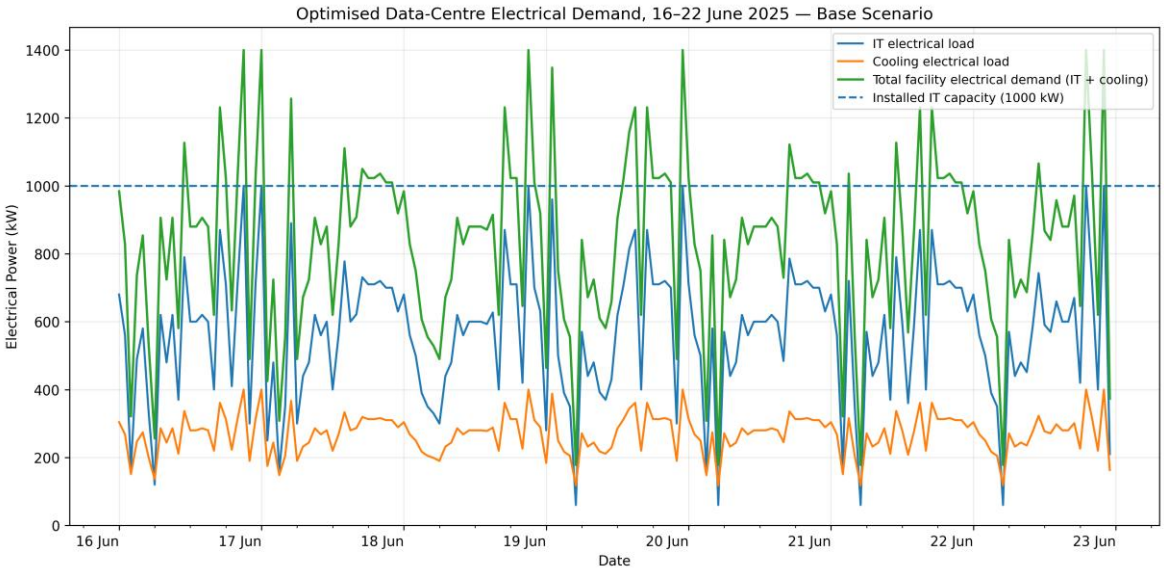

Figure 5.6. Optimized data-center electrical demand during a representative week in the base scenario.

As shown in Figure 5.6, the IT electrical load varies throughout the week rather than remaining constant. The dashed line represents the installed IT-capacity limit of 1000 kW, which is not exceeded by the scheduled workload. Cooling demand changes with the IT load according to the cooling formulation used in the model. Consequently, the total facility demand may exceed the IT-capacity limit because it includes both IT and cooling power.

The weekly profile also illustrates how the final model differs from the earlier fixed-load assumption: the installed capacity is an upper limit, whereas actual hourly IT demand is determined by workload arrivals and flexible-workload scheduling.

Figure 5.7 presents a representative 24-hour optimized power balance for the triple-renewable and triple-battery scenario on 19 March 2025.

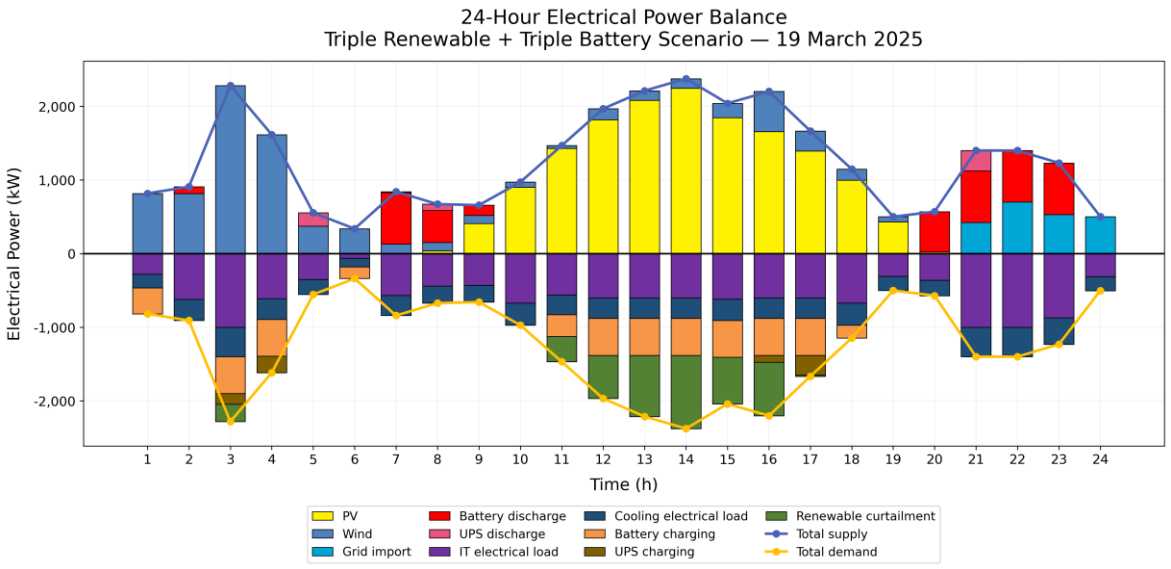

Figure 5.7. Representative 24-hour optimized electrical power balance for the triple-renewable and triple-battery scenario.

Figure 5.7 shows the hourly operation of renewable generation, grid electricity, battery and UPS operation, IT demand, cooling demand, storage charging and renewable curtailment. The optimizer adjusts these power flows while satisfying the hourly power balance and minimizing grid electricity import. Available renewable electricity may be supplied directly to the data-center load or used to charge the battery and UPS; any renewable generation that cannot be allocated is curtailed. The optimizer can also select battery and UPS discharge to help meet the data-center load.

Together, Figures 5.6 and 5.7 show that the model maintains the IT-capacity and power-balance requirements while coordinating time-varying data-center demand, renewable generation, and storage operation.

5.6 Model validation

The optimization results were checked to confirm that the main model constraints were satisfied. The validation includes the hourly power balance, renewable-power allocation, grid-import definition, IT-capacity limit, and completion of the flexible workload. Table 5.2 summarizes the maximum validation errors observed across the six simulation scenarios.

Table 5.2. Maximum numerical validation errors across the six simulation scenarios.

Validation check	What is verified	Maximum error
Power-balance check	Total power supply equals total data-center demand at each hour	0.000050000000 kW
Renewable-allocation check	Available renewable generation equals utilized renewable power plus curtailment	0.000067129995 kW
Grid-import check	Total grid import equals the sum of grid-to-load, grid-to-battery, and grid-to-UPS power flows	0.000000000000 kW
IT-capacity check	Scheduled IT power does not exceed the installed IT-capacity limit	0.000000000000 kW
Workload-completion check	Total scheduled flexible workload equals total flexible workload arrival over the simulation horizon	0.000080940314 kWh

As shown in Table 5.2, the maximum power-balance and renewable-allocation errors are below 0.0001 kW, while the grid-definition error and IT-capacity violation are zero. The maximum workload-completion error is approximately 0.000081 kWh, which is negligible compared with the annual flexible workload of 2,664,500 kWh. These very small numerical differences are consistent with solver tolerances. The validation therefore confirms that the optimized solutions satisfy the main power-flow, renewable-allocation, grid-import, IT-capacity, and workload-preservation requirements of the model.

Overall, the results show that increasing renewable capacity provides the largest reduction in grid electricity consumption, while additional battery capacity becomes more valuable when sufficient renewable surplus is available. Workload flexibility further improves renewable utilization and reduces curtailment under high-renewable conditions. The validation results confirm that these outcomes are obtained while satisfying the main operational constraints of the model.

6 Opportunities and challenges

The key opportunities and challenges that came out of the simulation results are identified in this chapter. The work focuses on how renewable generation, battery storage, UPS operation and workload flexibility can support more efficient and scalable data center energy management.

Chapter 5 results show that increasing renewable capacity can reduce grid electricity dependence, while battery storage and flexible workload scheduling can improve the use of available renewable energy. However, increased penetration of renewables can also lead to increased curtailment when storage and demand flexibility are limited. This chapter considers both the benefits and the practical limitations of scaling renewable-integrated data center systems.

6.1 Opportunities for efficient data center operation

The simulation results show several opportunities for improving data center energy operation. One of the clearest is the use of more on-site renewable generation. In this study, increasing PV and wind capacity reduced the amount of electricity required from the grid, showing that renewable integration can directly lower grid dependence.

Workload flexibility also provided a useful benefit. By shifting flexible IT tasks within the allowed delay window, the model was able to use more renewable electricity and reduce curtailment. This means that part of the data center demand can be moved to better match periods when renewable generation is available, without reducing the total computational work.

Battery storage provides an additional opportunity by retaining excess renewable electricity for use at a later time. The results further indicate that the benefit of increasing battery capacity depends on the amount of surplus renewable energy available. At the base renewable level, increasing battery capacity had only a small effect, while under higher renewable generation the larger battery became much more useful.

UPS also adds short-term flexibility because it can charge and discharge while maintaining its minimum reserve. Overall, the results suggest that the best operational benefit comes from coordinating renewable generation, storage, UPS operation, and flexible workload scheduling rather than relying on only one flexibility option.

6.2 Opportunities and challenges for system scalability

The results show that renewable capacity can be increased to reduce grid electricity use, but scaling the system is not only about adding more PV and wind. When renewable generation tripled, grid import dropped clearly, but curtailment also increased because not all the additional renewable energy could be used.

Battery scaling showed a different result. Increasing the battery capacity alone gave very little benefit at the base renewable level because there was not enough surplus renewable energy to make full use of the larger battery. However, when higher renewable capacity was combined with a larger battery, the storage system became much more useful and grid import decreased further.

This demonstrates that renewable generation and storage should be scaled together, not independently. Flexibility of the workload is also becoming more important at higher renewable levels, as it helps to shift demand to hours when more renewable energy is available. The main challenge is thus to find a balanced combination of renewable capacity, storage size and flexible demand in order to make sure that the added capacity can be used efficiently and not lost due to curtailment.

6.3 Challenges of renewable-integrated data center operation

The main challenge is that solar and wind generation are variable and depend on weather conditions. Even with higher installed renewable capacity, generation may still be low at some hours, so the data center continues to rely on the grid when renewable supply is insufficient.

Another challenge is the use of surplus renewable power. At high renewable penetration, curtailment may rise if the battery, UPS or flexible load cannot absorb the available power.

Storage can help, but its energy capacity and charging and discharging limits constrain how much energy can be shifted to later hours.

Workload flexibility also has practical limits. Flexible tasks can only be delayed within the allowed time window, and the total scheduled IT load must remain within the installed IT capacity. Therefore, workload shifting can improve renewable use, but it cannot solve every mismatch between generation and demand.

The model used in this thesis is also simplified. It does not include grid outages, backup generators, detailed cooling control, or geographical workload shifting. These aspects would need to be considered in more detailed real-world implementation.

6.4 Implications for efficient and scalable data center operation

The results show that renewable integration can reduce grid electricity use, but the benefit depends on how the different parts of the system are combined. Higher renewable capacity gives a clear reduction in grid dependence, but it can also increase curtailment when the additional generation cannot be used or stored. This implies that the addition of more renewable capacity does not necessarily mean that the system will perform better.

The battery results show a similar pattern. Increasing battery capacity alone gives only a small benefit when renewable surplus is limited. However, when renewable generation is higher, additional battery capacity can absorb more of the available surplus and thereby reduce dependence on grid electricity. Workload flexibility provides another useful option by shifting part of the IT demand to hours when renewable electricity is more available.

Overall, the study shows that efficiency and scalability are closely connected. A more efficient renewable-integrated data center is not achieved by scaling one component independently, but by balancing renewable capacity, storage capacity, and flexible demand. The main opportunity is therefore the coordinated use of these resources, while the main challenge is avoiding oversized renewable or storage capacity that cannot be used effectively. This balance is important when designing a data center energy system that can grow while still making good use of renewable electricity.

7 Conclusions

This chapter presents the principal conclusions of the study, discusses its limitations, and identifies directions for further investigation. The conclusions draw on the annual optimization results reported in Chapter 5 and the opportunities and challenges examined in Chapter 6.

7.1 Summary of findings

The study examined how renewable generation, energy storage, UPS operation, and flexible IT workloads can be coordinated to reduce a data center's dependence on grid electricity while supporting efficient and scalable operation.

The results show that increasing renewable capacity has the strongest effect on reducing grid electricity use. In the base optimized case, annual grid import was 5,686,400 kWh. When renewable generation was tripled, grid import decreased to 4,017,865 kWh, while the combined triple-renewable and triple-battery case achieved the lowest grid import of 3,680,360 kWh.

The results also indicate that battery capacity on its own does not necessarily offer a large benefit. Increasing the battery from 1200 kWh to 3600 kWh at the base renewable level reduced grid import by only about 0.10%. However, under triple renewable generation, the larger battery reduced grid import by about 8.40% and improved renewable utilization. This shows that storage capacity becomes more useful when enough renewable surplus is available.

Workload flexibility also improves the use of renewable energy. Under the triple-renewable condition, allowing a 3-hour workload-shifting window reduced grid import by about 4.29% compared with the no-shifting case. It also increased renewable utilization and reduced curtailment, while preserving the total computational workload.

In conclusion, the results suggest that renewable generation, storage capacity and workload flexibility are most effective when considered together. Increasing just one element is not always the best outcome. A mixed portfolio of renewable capacity, storage and flexible

demand is a better way to reduce grid dependence and increase renewable energy utilization with an eye to future system scaling. The validation results also verified that the optimized solutions met the major power-balance, renewable-allocation, grid-import, IT-capacity, and workload-preservation requirements of the model.

7.2 Study limitations

The findings should be interpreted in light of several limitations. The model provides a simplified representation of a data center rather than a complete model of an operating facility. The cooling system is also represented with an aggregated model connected to the IT load, not detailed cooling equipment.

The simulation is also for normal grid-connected operation. The analysis does not include the effects of grid outages and backup generators, electricity prices, economic costs, or carbon emissions. Workload flexibility is represented by using predefined hourly workload profiles and a maximum delay window, while renewable generation is based on weather data from a single simulation year.

The UPS is modeled as a controllable storage resource that must maintain a minimum energy reserve. This simplifies the reliability and operational requirements that would apply to UPS systems in real data centers. Therefore, the results should be understood as an assessment of the proposed energy-management framework rather than a complete representation of all real-world data center operating conditions.

7.3 Future research directions

Further work could build on this study by incorporating electricity prices and economic optimization, allowing operating costs to be evaluated alongside grid electricity consumption. The model could also be expanded to examine carbon emission impacts and compare the environmental benefits of different renewable and storage configurations.

Using measured workload data from a real data center would improve the representation of workload flexibility. A more detailed cooling model could also be included to study cooling

flexibility together with IT workload scheduling. Future work could further explore grid outages, backup generators and more detailed UPS reliability requirements.

The renewable-energy analysis can be improved by using weather data from multiple years instead of a single simulation year. Finally, a broader range of renewable and battery capacities can be investigated to discover optimal combinations for large-scale data center systems.

Overall, this thesis demonstrates that renewable energy can result in more efficient data center operation by reducing grid electricity use and increasing the utilization of available renewable generation. However, the results also indicate that the scalability depends on the combination of renewable capacity, storage capacity and flexible IT demand. Merely increasing one component does not necessarily produce the best result. A coordinated approach, where renewable generation, storage and workload flexibility are scaled together, presents a more effective path towards efficient and scalable renewable-integrated data center operation.

References

Aljabery, A.A.M., Mehrjerdi, H., Mahdavi, S. and Hemmati, R. (2021) 'Multi carrier energy systems and energy hubs: comprehensive review, survey and recommendations', *International Journal of Hydrogen Energy*, 46(46), pp. 23795–23814. Available at: https://doi.org/10.1016/j.ijhydene.2021.04.178.

Bhardwaj, R., Padmavathy, R., Preetha, M., Suresh, R., Kumar, Y., Dilip, S. and Tharmar, S. (2024) 'EMS for sustainable data centers', *E3S Web of Conferences*, 591, article 01006. Available at: https://doi.org/10.1051/e3sconf/202459101006.

CSI Solar Co., Ltd. (2024) *BiHiKu6: 530 W–555 W bifacial mono PERC, CS6W-530|535|540|545|550|555MB-AG* [Datasheet], version 2.91. Available at: https://static.csisolar.com/wp-content/uploads/sites/9/2024/07/24171839/CS-Datasheet-BiHiKu6_CS6W-MB-AG_v2.91_EN.pdf (Accessed: 29 July 2026).

Fan, H., Wang, C., Liu, L. and Li, X. (2022) 'Review of uncertainty modeling for optimal operation of integrated energy system', *Frontiers in Energy Research*, 9, article 641337. Available at: https://doi.org/10.3389/fenrg.2021.641337.

Finnish Meteorological Institute (FMI) (n.d.) *Download observations* [Data service]. Available at: https://en.ilmatieteenlaitos.fi/download-observations (Accessed: 21 May 2026).

He, W., Xu, Q., Liu, S., Wang, T., Wang, F., Wu, X., Wang, Y. and Li, H. (2024) 'Analysis on data center power supply system based on multiple renewable power configurations and multi-objective optimization', *Renewable Energy*, 222, article 119865. Available at: https://doi.org/10.1016/j.renene.2023.119865.

Jung, C. and Schindler, D. (2021) 'The role of the power law exponent in wind energy assessment: a global analysis', *International Journal of Energy Research*, 45(6), pp. 8484–8496. Available at: https://doi.org/10.1002/er.6382.

Mitra, P. (2025) 'Data center modeling and UPS performance' [PowerPoint presentation]. Electric Power Research Institute. Presented at the North American Electric Reliability Corporation Large Loads Task Force Meeting and Workshop, Austin, Texas, 10 April, pp.

19–28. Available at: https://www.nerc.com/comm/RSTC/LLTF/LLTF_April_Meeting_&_Technical_Workshop_Presentations_.pdf (Accessed: 29 July 2026).

Rickerson, W. (2025) 'Large loads and the changing grid: an ERCOT perspective' [PowerPoint presentation]. Electric Reliability Council of Texas. Presented at the North American Electric Reliability Corporation Large Loads Task Force Meeting and Workshop, Austin, Texas, 10 April, pp. 7–14. Available at: https://www.nerc.com/comm/RSTC/LLTF/LLTF_April_Meeting_&_Technical_Workshop_Presentations_.pdf (Accessed: 29 July 2026).

Seyfi, M., Mehdinejad, M., Mohammadi-Ivatloo, B. and Shayanfar, H. (2022) 'Scenario-based robust energy management of CCHP-based virtual energy hub for participating in multiple energy and reserve markets', *Sustainable Cities and Society*, 80, article 103711. Available at: https://doi.org/10.1016/j.scs.2022.103711.

SoltaniNejad Farsangi, A., Hadayeghparast, S., Mehdinejad, M. and Shayanfar, H. (2018) 'A novel stochastic energy management of a microgrid with various types of distributed energy resources in presence of demand response programs', *Energy*, 160, pp. 257–274. Available at: https://doi.org/10.1016/j.energy.2018.06.136.

Springer, T., Gravois, P. and Gibfried, J. (2025) 'White paper #2 update: assessment of gaps in existing practices, requirements and reliability standards for emerging large loads' [PowerPoint presentation]. Presented at the North American Electric Reliability Corporation Large Loads Task Force Meeting and Workshop, Austin, Texas, 10 April, pp. 125–133. Available at: https://www.nerc.com/comm/RSTC/LLTF/LLTF_April_Meeting_&_Technical_Workshop_Presentations_.pdf (Accessed: 29 July 2026).

Takcı, M.T., Qadrdan, M., Summers, J. and Gustafsson, J. (2025a) 'Data centres as a source of flexibility for power systems', *Energy Reports*, 13, pp. 3661–3671. Available at: https://doi.org/10.1016/j.egyr.2025.03.020.

Takcı, M.T., Day, J. and Qadrdan, M. (2025b) 'Characterisation and quantification of data centre flexibility for power system support', *arXiv* [Preprint], arXiv:2511.07159. Available at: https://arxiv.org/abs/2511.07159 (Accessed: 16 June 2026).

Villalva, M.G., Gazoli, J.R. and Ruppert Filho, E. (2009) 'Comprehensive approach to modeling and simulation of photovoltaic arrays', *IEEE Transactions on Power Electronics*, 24(5), pp. 1198–1208. Available at: https://doi.org/10.1109/TPEL.2009.2013862.

Wind-Turbine-Models.com (2023) *GE Vernova GE 1.5s: 1.50 MW wind turbine* [Online datasheet]. Available at: https://en.wind-turbine-models.com/turbines/565-ge-vernova-ge-1-5s (Accessed: 29 July 2026).

Zhang, X., Lindberg, T., Svensson, K., Vyatkin, V. and Mousavi, A. (2016) 'Power consumption modeling of data center IT room with distributed air flow', *International Journal of Modeling and Optimization*, 6(1), pp. 33–38. Available at: https://doi.org/10.7763/IJMO.2016.V6.499.

Zhao, M. and Wang, X. (2021) 'A synthetic approach for datacenter power consumption regulation towards specific targets in smart grid environment', *Energies*, 14(9), article 2602. Available at: https://doi.org/10.3390/en14092602.